Chapter 7

Neoproterozoic glacial palaeolatitudes: a global update

D. A. D. EVANS[1]* & T. D. RAUB[2]

[1]*Department of Geology & Geophysics, Yale University, 210 Whitney Avenue, New Haven, CT 06520-8109, USA*

[2]*Division of Geological and Planetary Sciences, 100-23 Caltech, Pasadena CA 91125, USA*

*Corresponding author (e-mail: dai.evans@yale.edu)

Abstract: New stratigraphic, geochronological and palaeomagnetic constraints allow updates to be made to a synthesis of Neoproterozoic glacial palaeolatitudes, including modifications to some reliability estimates. The overall pattern of a Neoproterozoic climatic paradox persists: there is an abundance of tropical palaeolatitudes and near to complete absence of glaciogenic deposits demonstrably laid down between latitudes of 60° and 90°. In addition to 12 units with palaeolatitude estimates that are somewhat reliable, estimates with moderate to high reliability now include Konnarock (less than 10° from the palaeo-equator), Elatina, Rapitan, Mechum River, Grand Conglomerat (10–20°), Upper Tindir, Puga (20–30°), Nantuo, Gaskiers (30–40°) and Walsh (40–50°). Among these, Elatina, Upper Tindir and Nantuo are considered to have the highest reliability, all with estimates of low to moderate palaeolatitude. The Elatina result stems from sedimentary rocks with quantitative correction of inclination-shallowing effects, and the Upper Tindir result stems from data collected from igneous rocks that are precisely coeval with the glacial deposits. Despite continuing debate on the global character of Neoproterozoic ice ages, their pan-glacial extent (ice extending to low latitude in a low-obliquity world) is well demonstrated.

Palaeomagnetism of glaciogenic deposits has provided a quantitative basis for hypotheses of extreme climatic shifts in the late Neoproterozoic Era. The most recent global compilations of palaeomagnetic depositional latitudes for Proterozoic ice ages indicate a dominant mode near the palaeo-equator (Evans 2000, 2003), with no robust palaeo-polar deposits yet discovered. Such results could therefore support either the Snowball Earth (Kirschvink 1992) or the high-obliquity (Williams 1993) hypotheses for Precambrian ice ages, but would appear to reject the uniformitarian comparison to polar/temperate-restricted Phanerozoic glaciogenic deposits (Evans 2000). Hoffman (2009) has suggested that Neoproterozoic ice ages represent a globally all-encompassing 'pan-glacial' state of the Earth's climate system, fundamentally distinct from either partially ice-covered 'glacial–interglacial' or ice-free 'nonglacial' palaeoclimates experienced during the Phanerozoic Eon.

Several reviews of stratigraphic (Halverson *et al.* 2005, 2007), sedimentological (Hoffman & Schrag 2002; Eyles & Januszczak 2004; Fairchild & Kennedy 2007; Hoffman *et al.* 2007; Allen & Etienne 2008; Hoffman 2009) and palaeomagnetic (Trindade & Macouin 2007; Hoffman & Li 2009) data sets pertaining to Neoproterozoic ice ages have appeared recently. These discussions of glacial deposits owe much to the pioneering synthesis of Hambrey & Harland (1981), but the recent reviews arrive at differing conclusions regarding the extent and severity of Neoproterozoic ice ages. In particular, the study by Eyles & Januszczak (2004) is commonly cited as a palaeogeographic alternative that avoids the need for nonuniformitarian processes to account for the advance of widespread continental ice sheets into tropical palaeolatitudes. It becomes useful, then, to review the global evidence for or against low-latitude glaciation. Herein, we reassess Neoproterozoic glacial palaeolatitudes in light of new stratigraphic, geochronological and palaeomagnetic data obtained within the last decade, providing the first comprehensive update and revision of the palaeographic analyses of Evans (2000).

Methods

Table 7.1 lists the known or alleged Neoproterozoic glaciogenic deposits, revising the unit-identifying numbering scheme introduced by Evans (2000), but with cross-references to that study, as well as those of Hambrey & Harland (1981), Eyles & Januszczak (2004, table 1), Trindade & Macouin (2007) and Hoffman & Li (2009). Deposits are numbered by present geographical location, differentiating units that are separated from each other on the scale of 100 km or more, or in some cases distinguishing units of uncertain relative correlation that are presently adjacent via tectonic stacking in orogenic belts. Within each numbered location, the units are denoted (a, b, c, etc.) in ascending stratigraphic order. Many global chronostratigraphic schemes have been proposed, that assign ages to undated deposits via correlation, but herein, we adopt the approach used by Evans (2000) to consider each unit's age constraints in isolation. This splitting, rather than lumping, approach serves to illustrate how few of the deposits are precisely dated or studied palaeomagnetically. Many of the deposits have been classified using the loose terms 'Sturtian', 'Marinoan', or 'Ediacaran' based on the lithographic character of either diamictites or their overlying cap carbonates (e.g. Hoffman & Li 2009). Recent U–Pb geochronology has thus far permitted many so-called Marinoan deposits to record the synchronous end of a widespread ice age of unknown duration, which ended at 635 Ma (Hoffmann *et al.* 2004; Condon *et al.* 2005; Zhang *et al.* 2008), and a mid-Ediacaran ice age at *c.* 580 Ma (Bowring *et al.* 2002, abstract only). U–Pb ages of so-called Sturtian deposits range from *c.* 765 Ma (Key *et al.* 2001) to possibly as young as *c.* 660 Ma (Fanning & Link 2008; from the type area in South Australia). Use of the lithological characteristics of cap carbonates as global correlation tools appears successful in some instances, but may be problematic in others (Corsetti & Lorentz 2006; Kendall *et al.* 2009).

Finally, several of the units discussed by Evans (2000) are now considered irrelevant to discussions on Neoproterozoic ice ages, as they are likely nonglacial, or demonstrably Cambrian or younger in age. Those units are included in Table 7.1, but are now stripped of their numerical codes. In a few cases, questions remain about these issues, and the deposits retain their numerical status until documented otherwise.

Table 7.1 also lists our preferred interpretation on the reliability of palaeolatitude determination for the deposits, using the three-level qualitative scale after Evans (2000). Although quantitative measures of palaeomagnetic pole reliability exist (e.g. Van der Voo 1990), they have generally been tailored towards plate reconstructions rather than palaeoclimatic problems. Herein, we regard

Table 7.1 *Published assessments of glacial influence and depositional palaeolatitude for Neoproterozoic strata*

#	Deposit name	Lat (°N)	Long (°E)	HH81	E00	EJ04	TM07	HL09	This study
Laurentia and environs									
1a	Hula Hula	69.5	215.5	–	–	–	–	Hu(S) 0–15	No pmag data
1b	Katakturuk unit 2	69.5	214.5	–	–	–	–	–	No pmag data
2a	Upper Tindir: unit 2	65	222	Yes (F10)	No pmag data (#3)	–	–	Ti(S) 0–15	*** 21 ±3
2b	Upper Tindir: unit 3b	65	219	–	–	–	–	–	No pmag data
3a	Rapitan	64	230	Yes (F11)	** 06 +8/−7 (#1)	Yes	Q = 4; 06 ±4	Ra(S) 0–15	** 18 ±3
3b	Ice Brook (Stelfox)	63.5	231.5	–	Unreliable pmag (#2)	??	–	IB(M) 0–15	Unreliable pmag
4	Mt Lloyd George	58	235	Yes (F12)	No pmag data (#4)	–	–	–	No pmag data
5	Deserters Range	57	235.5	–	No pmag data (#4)	–	–	–	No pmag data
6	Mount Vreeland	54.5	239	Uncertain (F12)	No pmag data (#5)	–	–	Vr(M) 0–15	No pmag data
7	Toby	49.5	243	Yes (F13)	* 08 ±4 (#6)	–	–	To(S) 0–15	No pmag data
8	Edwardsburg	45	244.5	–	No pmag data (#7)	–	No pmag data	–	No pmag data
9	Pocatello: Scout Mtn	42.5	248	Yes (F14)	No pmag data (#7)	–	Q = 6; 08 ±3	Po(S) 0–15	No pmag data
10	Mineral Fork/Dutch Pk	40.5	247.5	Yes (F15)	No pmag data (#7)	–	–	–	No pmag data
11a	Kingston Peak: Surprise	36	243.5	Yes (F16)	No pmag data (#8)	No	–	Su(S) 0–15	No pmag data
11b	Kingston Peak: Wildrose	36	243.5	–	No pmag data (#8)	No	–	Wr(M) 0–15	No pmag data
11c	Ibex	36	243.5	–	–	–	–	–	No pmag data
11d	Johnnie Rainstorm	36	244	–	* 01 ±4 (#9)	–	–	–	* 01 ±4
12	Cerro Las Bolas	29	250.5	–	–	–	–	–	No pmag data
–	Florida Mtns	32	252.5	Yes (F17)	* 03 ±8 (#10)	–	–	–	Too young
13	Konnarock/Grandf. Mtn	36.5	278.5	Yes (F18)	See Mechum R (#11)	No	–	Kn(S) 15–30	** 06 ±5
14a	Mechum River	38.5	281.5	–	** 20–21 ±4 (#11)	–	–	–	** 16 ±3
14b	Fauquier	39	282.5	–	–	–	–	–	* 78 ±12
15a	Port Askaig	55.5	353.5	Yes (E18–E20)	Unreliable pmag (#12)	Yes	No pmag data	Pt(S) 30–45	Unreliable pmag
15b	Stralinchy (Reelan)	55.5	353.5	–	–	–	–	Re(M) 30–45	No pmag data
15c	Loch na Cille	55.5	353.5	–	No pmag data (#12)	–	–	Lo(E) 75–90	Unreliable pmag
16	Gåseland/Charcot Land	71	330.5	Yes (F23,F24)	No pmag data (#14)	–	–	–	No pmag data
17a	Tillite Gp: Ulvesø	73	336	Yes (F25)	Unreliable pmag (#15)	Yes	–	Ul(S) 15–30	Unreliable pmag
17b	Tillite Gp: Storeelv	73	336	Yes (F25)	Unreliable pmag (#15)	Yes	–	St(M) 30–45	Unreliable pmag
18a	Elbobreen (Petrovbreen)	79.5	18	Yes (E10)	No pmag data (#16)	–	–	Pb(S) 15–30	No pmag data
18b	Wilsonbreen	79.5	18	Yes (E10)	No pmag data (#16)	–	–	Wb(M) 30–45	No pmag data
19	West Spitsbergen	78	13	Yes (E10)	No pmag data (#17)	–	–	–	No pmag data
20	Moraenesø	82	326	Yes (F26)	No pmag data (#18)	–	–	–	No pmag data
21	Pearya	82.5	281.5	–	No pmag data (#19)	–	–	–	No pmag data
Baltica									
22a	Vestertana: Smalfjord	70	28	Yes (E12)	** 33 +14/−12 (#20)	Yes (a or b)	Q = 3; 33 ±9	Sm(M) 45–60	* 33 +14/−12
22b	Vestertana: Mortensnes	70	28	Yes (E12)	** 33 +14/−12 (#20)	Yes (a or b)	Q = 3; 33 ±9	Mt(E) 45–60	No pmag data
–	Sito/Vakkejokk	68	19	Uncertain (E13)	Too young (#21)	–	–	–	Too young
23	Långmarkberg/Lillfjället	64	14.5	Yes (E14/E15)	No pmag data (#22)	–	–	–	No pmag data
24	Moelv	61.5	11	Yes (E16)	Unreliable pmag (#23)	Yes	No pmag data	Mo(E) 45–60	Unreliable pmag
25	Vilchitsy/Blon	53	32	Yes (E24–E28)	Unreliable pmag (#24)	–	–	Vi(E) 45–60	Unreliable pmag
26	N Urals: Churochnaya	60	57.5	Yes (E30)	No pmag data (#25)	–	–	Cn(E) 30–45	No pmag data
27a	C Urals: Tany	58.5	59	Yes (E31)	No pmag data (#26)	–	–	Ty(S) 45–60	No pmag data

27b	C Urals: Koyva	58.5	59	Yes (E31)	No pmag data (#26)	–	–	–	No pmag data
27c	C Urals: Staryye Pechi	58.5	59	Yes (E31)	No pmag data (#26)	–	–	–	No pmag data
28	S Urals: Kurgashlya	53.5	57.5	Yes (E32)	Unreliable pmag (#27)	–	–	–	Unreliable pmag
Altaids and Siberia									
29a	West Altaids (Satan/Dzhetym)	44	72	Yes (C27)	No pmag data (#31)	–	–	–	No pmag data
29b	West Altaids (Baykonur)	44	72	Variable (C22–C28)	No pmag data (#31)	–	–	Br(S) 45–60	No pmag data
30a	Tsagaan Oloom (Maikhan Ul)	47	96	–	No pmag data (#32)	Blank	–	Mk(S) 0–15	Unreliable pmag
30b	Tsagaan Oloom (Khongoryn)	47	96	–	–	–	–	Kg(M) 0–15	* 03 ± 11
31	East Sayan/Khubsugul: Zabit	51	100	–	No pmag data (#30)	–	–	–	Unreliable pmag
32a	Chivida	61	92	Nonglacial (C30)	Unreliable pmag (#28)	–	–	Cv(S) 15–30	Unreliable pmag
32b	Pod'em	61	92	–	–	–	–	Pd(M) 0–15	No pmag data
33	Marnya	54.5	99	–	–	–	–	Ma(M) 0–15	No pmag data
34a	Patom: Kharluktakh	59	115	–	–	–	–	Kh(S) 0–15	No pmag data
34b	Patom: Dzhemkukan	59	115	Uncertain (C31)	No pmag data (#29)	–	–	Dz(M) 0–15	No pmag data
China cratons									
35a	Aksu: Qiaoenbrak	41	79.5	Yes (C33)	* 08 ±8 (#33)	–	–	–	No pmag data
35b	Aksu: Yuermeinbrak	41	79.5	Yes (C33)	* 08 ±8 (#33)	–	–	–	* 27 ± 9
36a	Quruqtagh: Bayisi	41.5	87.5	Yes (C33)	* 08 ±8 (#33)	–	Q = 4; 01 ±3	By(S*) 30–45	* 01 +4/−2
36b	Quruqtagh: Tereeken	41.5	87.5	Yes (C33)	* 08 ±8 (#33)	–	–	Te(M) 15–30	No pmag data
36c	Quruqtagh: Hankalchough	41.5	87.5	Yes (C33)	* 08 ±8 (#33)	–	–	Ha(E) 15–30	No pmag data
37	Qaidam: Hongtiegou	37.5	96	Yes (C33)	–	–	–	–	No pmag data
38	Luoquan	34	115	Yes (C33,C34)	Unreliable pmag (#34)	Yes	–	Lq(E) 0–15	Unreliable pmag
39a	Chang'an/Tiesiao/Jiangkou	27	111	Yes (C33,C35)	*** 30–40 ±12 (#35)	Yes (a or b)	–	Ji(S) 15–30	No pmag data
39b	Nantuo	27	111	Yes (C33,C35)	*** 30–40 ±12 (#35)	Yes (a or b)	Q = 6; 04 ±4	Na(M) 15–30	*** 37 ±9
India to Nubia									
40	Blaini	30	78.5	Yes (C14)	Unreliable pmag (#37)	–	–	Bl(M) 0–15	Unreliable pmag
–	Penganga	19.5	75	–	No pmag data (#38)	–	–	–	Nonglacial
41	Rizu	31	56	–	–	–	–	Ri(M) 0–15	Too young?
42a	Ghubrah	23	58	–	Unreliable pmag (#36)	–	No pmag data	Gu(S) 15–30	No pmag data
42b	Fiq	23	58	–	No pmag data (#36)	Yes ('Shuram')	Q = 6; 15 ±4	Fi(M) 30–45	* 13 ±7
43a	Ayn	17.5	55	–	Unreliable pmag (#36)	–	–	Ay(S) 15–30	Unreliable pmag
43b	Shareef	17.5	55	–	No pmag data (#36)	–	–	Sh(M) 30–45	* 18 ±7
44	Tambien	14	39	–	–	–	–	Ta(S) 15–30	No pmag data
45	Atud	26	35	–	–	–	–	–	No pmag data
Australia and Mawsonland									
46	Walsh	−17	126	Yes (D16)	** 45 +14/−12 (#42)	–	Q = 5; 45 ±5	–	** 45 +14/−12
47a	Landrigan	−18	126.5	Yes (D16)	No pmag data (#44)	–	–	La(M) 0–15	No pmag data
47b	Egan	−18.5	126.5	Yes (D16)	* 21 ±8 (#43)	–	–	Eg(E) 15–30	* 21 ±8
48a	Fargoo	−17	129	Yes (D16)	No pmag data (#44)	–	–	–	No pmag data
48b	Moonlight Valley	−17	129	Yes (D16)	No pmag data (#44)	Yes	–	–	No pmag data
49	Little Burke	−21.5	140	Yes (D19)	Unreliable pmag (#40)	–	–	–	Unreliable pmag
50a	Areyonga/Naburula/Yardida	−23	134	Yes (D17,D18)	No pmag data (#39)	–	–	Ar(S) 15–30	No pmag data
50b	Olympic/Mount Doreen	−23	135	Yes (D17)	No pmag data (#40)	–	–	Ol(M) 0–15	No pmag data

(*Continued*)

Table 7.1 *Continued*

#	Deposit name	Lat (°N)	Long (°E)	HH81	E00	EJ04	TM07	HL09	This study
51	Boondawari/Wahlgu/Turkey Hill	−25	124	–	No pmag data (#40)	–	–	–	Unreliable pmag
52	Chambers Bluff	−27	134	–	No pmag data (#39)	–	–	–	No pmag data
53a	Sturtian (type area)	−32	139	Yes (D21)	Unreliable pmag	Yes	No pmag data	St(S) 0–15	Unreliable pmag
53b	Elatina	−32	139	Yes (D21)	*** 03–09 ±4 (#40)	Blank	Q = 4,6; 05 ±6	El(M) 0–15	*** 10–14
54a	Yancowinna	−31.5	141.5	Yes (D20)	No pmag data (#39)	–	–	–	No pmag data
54b	Teamsters Creek	−31.5	141.5	Yes (D20)	No pmag data (#40)	–	–	–	No pmag data
55	Cottons	−40	144	Uncertain (D22)	Unreliable pmag (#41)	–	No pmag data	Co(M) 0–15	Unreliable pmag
56a	Julius River	−41	145	Uncertain (D22)	No pmag data (#41)	–	No pmag data	Ju(S) 0–15	No pmag data
56b	Croles Hill	−40.5	145	–	–	–	No pmag data	Cr(E) 0–15	No pmag data
57	Goldie	−83	160	–	No pmag data (#45)	–	–	–	No pmag data
	Kalahari and environs								
58a	Blaubeker/Court	−23.5	17.5	Yes (A29)	Unreliable pmag (#46)	–	–	Bb(S) 0–15	Unreliable pmag
58b	Blasskrans/Naos	−23.5	17.5	Map only (A29)	No pmag data (#47)	–	–	Bk(M) 0–15	No pmag data
59a	Kaigas	−28.5	16.5	Nonglacial (A29)	No pmag data (#48)	–	No pmag data	Ka(S*) 0–15	No pmag data
59b	Numees	−28.5	16.5	Yes (A29)	No pmag data (#49)	–	–	Nu(M) 0–15	No pmag data
59c	Namaskluft	−28.5	16.5	Yes (A29)	No pmag data (#49)	–	–	0–15	No pmag data
59d	Schwarzrand	−27	18	Yes (A29)	* 38 ±3 (#51)	–	–	–	* 38 ±3
60a	Karoetjes Kop	−31.5	18.5	–	–	–	–	–	No pmag data
60b	Aties	−32	18.5	Nonglacial (A29)	No pmag data (#50)	–	–	–	No pmag data
61	Dernburg	−28	15.5	–	–	–	–	–	No pmag data
	Congo-São Francisco								
62a	Grand Conglomérat	−11	27	Yes (A28)	No pmag data (#52)	–	Q = 5; 10 ±6	Gr(S*) 15–30	** 10 ±5
62b	Petit Conglomérat	−11	27	Uncertain (A28)	No pmag data (#53)	–	–	Pe(M) 0–15	No pmag data
63	Geci	−13	35	–	–	–	–	–	No pmag data
64	Tshibangu	−2	29	–	No pmag data (#54)	–	–	–	No pmag data
65	Bunyoro	1.5	31.5	Yes (A25)	No pmag data (#55)	–	–	–	No pmag data
66a	Akwokwo/Bandja	3	24	–	No pmag data (#55)	–	–	Ak(S) 30–45	No pmag data
66b	Bondo	5	20	–	No pmag data (#56)	–	–	Bo(M) 15–30	No pmag data
67	Mintom	3	13	–	–	–	–	–	No pmag data
68a	Sergipe: Juetê/Ribeirópolis	−11	322	–	No pmag data (#56)	–	–	–	No pmag data
68b	Sergipe: Palestina	−11	322	–	No pmag data (#56)	–	–	Pa(M) 30–45	No pmag data
69	Bebedouro	−11	319	Uncertain (G28)	No pmag data (#58)	–	–	–	Unreliable pmag
70	Rio Preto: Canabravinha	−11	314	–	–	–	–	–	No pmag data
71	Brasilia int: Ibiá/Cristalina	−18	313	Uncertain (G27)	No pmag data (#59)	–	–	–	No pmag data
72a	Vazante: St. Antônio do Bonito	−17.5	313	–	–	–	–	–	No pmag data
72b	Vazante: Lapa	−17.5	313	–	–	–	–	–	No pmag data
73	Carandaí	−21	316	Uncertain (G30)	No pmag data (#60)	–	–	–	No pmag data
74a	Bambui: Jequitaí/Macaúbas	−17	316	Yes (G31)	Unreliable pmag (#57)	No	–	Je(S) 30–45	Unreliable pmag
74b	Bambui: Inhaúma	−19.5	315.5	–	–	–	–	–	No pmag data
74c	Bambui: Lagoa Formosa	−18.5	313.5	–	–	–	–	–	No pmag data

No.	Name	Lat	Long	HH81/EJ04	E00		TM07	HL09	This study
75	Rio Pardo: Salobro	−15.5	320.5	Uncertain (G29)	Uncertain glacial (#57)	–	–	–	Nonglacial
76a	West Congo Inférieure	−5	14	Nonglacial (A26,A27)	No pmag data (#61)	–	–	In(S) 30−45	No pmag data
76b	West Congo Supérieure	−5	14	Nonglacial (A26,A27)	No pmag data (#62)	–	–	Sp(M) 15−30	No pmag data
77a	Chuos/Varianto	−21	16	Variable (A29)	* 10 ±5 (#63)	No	–	Ch(S) 15−30	* 09 ±5
77b	Ghaub	−21	16	Uncertain (A29)	Unreliable pmag (#64)	No	No pmag data	Gh(M) 0−15	Unreliable pmag

West Africa and Hoggar

No.	Name	Lat	Long	HH81/EJ04	E00		TM07	HL09	This study
78a	Basal Atar Gp	22	352	–	Unreliable pmag (#66)	–	–	–	Nonglacial?
78b	Jbéliat/Bthaat Ergil (triad)	22	352	Yes (A19)	* 30−70 (#65)	Yes	–	Jb(M) 45−60	No pmag data
79	Mali Gp/Bakoye	15	351	Yes (A19)	Same as #65 (#67)	–	–	Ba(M) 30−45	No pmag data
80	Rokel River	8.5	348	Yes (A20)	No pmag data (#68)	–	–	–	No pmag data
81a	Kodjari	10	0	Yes (A21)	No pmag data (#69)	–	–	Ko(M) 30−45	No pmag data
81b	Tamale/Obosum	8	0	Yes (A21)	No pmag data (#70)	–	–	–	No pmag data
82a	Série Verte (Tafeliant)	21	2	Yes (A23)	Unreliable pmag (#71)	–	–	–	Unreliable pmag
82b	Série Pourprée	24	2	Yes (A22)	Same as #65 (#72)	–	–	–	No pmag data
83	Série Tirririne	21	8.5	Yes (A23)	Unreliable pmag (#71)				Unreliable pmag
84a	Sarhro	31	352.5	–	No pmag data (#73)	–	–	–	No pmag data
84b	Tiddiline	30	352	Nonglacial (A18)	No pmag data (#73)	–	–	–	Unreliable pmag

Avalonia and Cadomia

No.	Name	Lat	Long	HH81/EJ04	E00		TM07	HL09	This study
85	Squantum	42.5	289	Uncertain (F19)	* 55 +8/−7 (#74)	No	Q = 3; 55 ±3	Sq(E) 75−90	* 55 +8/−7
86	Gaskiers	47.5	307	Yes (F20)	* 31 +10/−8 (#75)	Yes	No pmag data	Ga(E) 75−90	** 34 +8/−7
87	Gwna/Mona	53	355.5	–	–	–	–	–	No pmag data
88	Brioverian (Granville)	48.5	358	Nonglacial (E21)	No pmag data (#76)	No	–	Gr(E) 45−60	No pmag data
89	Clanzschwitz/Weesenstein	51	13.5	Correlative to (E22)?	–	–	–	–	No pmag data

Amazonia and environs

No.	Name	Lat	Long	HH81/EJ04	E00		TM07	HL09	This study
90a	Puga	−15.5	303	Yes (G26)	No pmag data (#77)	–	Q = 5; 22 ±6	Pu(M) 30−45	** 22 +6/−5
90b	Serra Azul	−15.5	303	–	–	–	–	Az(E) 60−75	No pmag data
91	Chiquerío	−15.5	285	–	No pmag data (13)	–	–	Cq(S) 15−30	No pmag data

Rio Plata and environs

No.	Name	Lat	Long	HH81/EJ04	E00		TM07	HL09	This study
92a	Zanja del Tigre	−34.5	305	–	–	–	–	–	Nonglacial?
92b	Las Ventanas/Playa Hermosa	−34.5	305	–	–	–	–	–	Unreliable pmag
93	Picada das Graças	−31	305.5	–	Unreliable pmag (#78)	–	–	–	Unreliable pmag
94	Iporanga	−24.5	311.5	–	–	–	–	–	No pmag data
95	Sierra del Volcán	−38	302	–	–	–	Q = 5; 48 ±7	–	Too young?

Deposits are numbered by geographical area; within each region, they are lettered by ascending stratigraphic order. Glaciogenic influence assessments: HH81, Hambrey & Harland (1981); EJ04, Eyles & Januszczak (2004, table 1). The terms 'yes', 'no' and 'uncertain' refer to the question of whether a glaciogenic influence has been demonstrated according to each compilation. 'Blank' refers to blank entries in Eyles & Januszczak (2004, table 1). Palaeomagnetic constraint assessments: E00, Evans (2000); TM07, Trindade & Macouin (2007); HL09, Hoffman & Li (2009). Correlations by Hoffman & Li (2009) presented in parentheses, follow the deposit abbreviations used in their work: E, Ediacaran; M, Marinoan; S, Sturtian; S*, nominally Sturtian but with possibly older ages than the deposits labelled 'S'. Asterisks in the columns for E00 and this study indicate the relative reliability (*, low; **, moderate; ***, high) of glacial palaeolatitudes assessed by Evans (2000) or herein. *Q* values use the reliability scheme of Van der Voo (1990). Throughout the table, dashed entries indicate that the deposit was not mentioned by the particular compilation.

reliability of glacial palaeolatitudes to depend mainly on the quality of palaeomagnetic data, but also on the confidence in chrono/lithostratigraphic correlations, if necessary for palaeolatitude estimation, and to a lesser extent the amount of consensus on the glaciogenicity of the deposits. In addition, some of our assessments in Table 7.1 are labelled 'unreliable pmag [palaeomagnetic data]', which merely indicates that the data are not applicable for reliable estimates of glacial palaeolatitude, although in some cases they could be useful for other purposes such as tectonic reconstructions. We do not provide references to all the stratigraphic, geochronological, and palaeomagnetic constraints on the deposits, but rather only discuss those instances in which our current assessment differs from previously published global compilations. Our global palaeolatitude estimates for Neoproterozoic ice ages, using this quality filtering method, are summarized graphically in Fig. 7.1.

We begin with the assumption that Earth's time-averaged ($>10^3$ years) magnetic field has the geometry of a geocentric-axial dipole (GAD). This assumption is justified to first order by the comparison of evaporite palaeolatitudes in the palaeomagnetic reference frame, relative to their expected palaeolatitudes according to intertropical convergence of zonal atmospheric circulation. Agreement between these two reference frames for most Proterozoic evaporite deposits implies that the GAD hypothesis is tenable for most of the last two billion years (Evans 2006). Departures from this model are possible, due to data gaps, over intervals as long as 100–200 million years; notably, the Neoproterozoic glacial interval does indeed lack voluminous evaporite deposits. Ephemeral, dominantly non-GAD fields (on the order of 10 million years duration or shorter) are also permissible, as will be discussed further below, but in light of the broader record of a uniformitarian geodynamo (see also Swanson-Hysell et al. 2009), a burden of proof must lie with these alternatives for any specific age.

Palaeomagnetic constraints on Neoproterozoic glacial palaeolatitudes

Laurentia and environs

Macdonald et al. (2010a) have produced direct, high-precision, U–Pb age constraints on the Upper Mount Harper Group diamictite-bearing succession, at 716.5 Ma, which is precisely coeval with the immediately underlying Mount Harper Volcanic Complex and the transcontinental Franklin large igneous province. The latter has yielded a high-quality palaeomagnetic pole representing data measured in several laboratories and spanning the width of Arctic Canada plus northwestern Greenland (Denyszyn et al. 2009). The Mount Harper and underyling Fifteenmile groups are well correlated, lithostratigraphically, to the Tindir Group across the length of the Oglivie Mountains, and the Franklin palaeomagnetic pole implies a depositional palaeolatitude of $21 \pm 3°$ for the Tindir/Mount Harper glaciogenic succession. We assign this result to the highest reliability in the present analysis, and it is noteworthy by the fact that it derives from igneous rocks that are immune from any possible effects of systematic inclination shallowing. We assign only slightly less reliability to the application of the Franklin mean palaeomagnetic pole to the Rapitan glaciogenic deposits in the adjacent Mackenzie Mountains (implied depositional palaeolatitude of $18 \pm 3°$) because that succession lacks the volcanic manifestation of the Franklin event. Correlation among the Upper Tindir, Upper Mount Harper and Rapitan diamictite successions is moderately strong, because of their close associations with Fe formation, similarity of overlying shale units, and reasonable matches of chemostratigraphic profiles from underlying units (Macdonald et al. 2010a). The palaeolatitudes determined herein for these deposits are slightly higher (c. 20°) than the previous estimate (06 +8/−7°; Evans 2000),
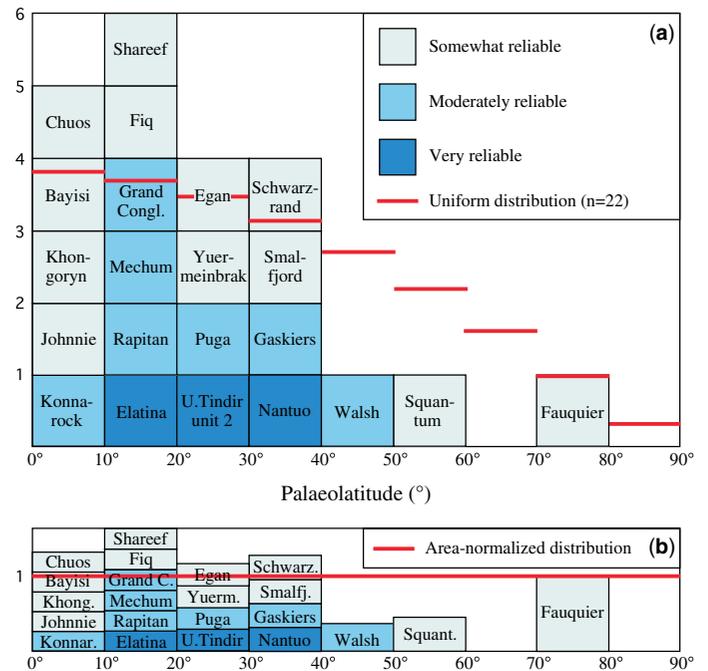

Fig. 7.1. Reliability of palaeomagnetic depositional latitudes for Neoproterozoic glacial deposits. (a) Unit-weight given to each estimate, following Evans (2000). Thick lines indicate the normalized probability at each latitude band, for a uniform (random) distribution over the surface of the Earth. (b) Latitude band-area normalization of the palaeolatitude estimates.

which was determined by direct measurements of the Rapitan succession that apparently were substantially affected by sedimentary inclination shallowing (implied flattening factor, $f \approx 0.3$ calculated here; see Tauxe et al. 2008). Nonetheless, general concordance of 750–700 Ma palaeomagnetic results from Laurentia (Fig. 7.2) indicates that the Earth's geomagnetic field was stable at that time. Distinctly higher in the Tindir stratigraphy, a second diamictite level (unit 3b) and overlying cap carbonate bear striking resemblance to the Stelfox/Ravensthroat diamictite/cap carbonate couplet in the nearby Mackenzie Mountains (Macdonald et al. 2010b). Neither of the younger diamictite/cap carbonate pairs at the two localities have palaeomagnetic constraints on depositional palaeolatitude.

Inliers on Alaska's North Slope belong to an Arctic Alaska–Chukotka microplate of questionable Laurentian or Siberian affinity. Regionally, diamictite (informally named Hula Hula) lies above post-760 Ma volcanic rocks, and locally, it is interbedded with basaltic flows (Macdonald et al. 2009a). The overlying Katakturuk dolomite contains a diagnostic unit (Katakturuk 2) considered correlative to classic Marinoan cap carbonates elsewhere in the world. Although the Hula Hula-associated flows might correlate to the Franklin event and merit application of that palaeomagnetic pole, the allochthonous nature of the terrane and uncertain timing and style of its accretion to Alaska render these deposits palaeomagnetically unconstrained.

New U–Pb ages on zircon from Neoproterozoic successions in Idaho support several distinct pulses of glaciation in that region. In the Pocatello region, Fanning & Link (2004) produced U–Pb SHRIMP ages constraining the Scout Mountain Member (mainly diamictite) of the Pocatello Formation, to slightly younger than 709 ± 5 Ma and substantially older than 667 ± 5 Ma. The younger age was determined using a zircon subpopulation from a channelized tuff horizon that lies closely beneath a crystal fan-bearing marble. The fans resemble those in post-glacial cap carbonates. It was suggested that the Scout Mountain Member represents a distinct glacial event from the Edwardsburg metadiamictites dated by Lund et al. (2003) at c. 685 Ma. More recently, however, the older age has been 'corrected' to 686 ± 4 Ma by
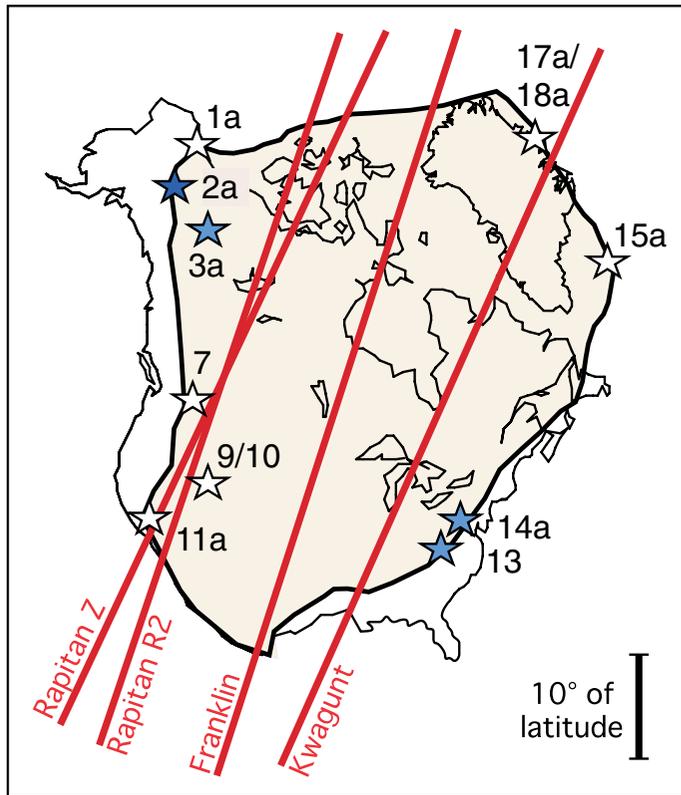
Fig. 7.2. Palaeoequators plotted across Laurentia, according to the named palaeomagnetic poles from 750 to 700 Ma, as discussed in the text and in Evans (2000). Numbered stars correspond to glaciogenic deposits keyed to Table 7.1. Star colours are keyed to the reliability scheme of Figure 7.1, or if uncoloured, stars represent deposits typically correlated with the Rapitan glaciation. References to palaeoequators given in Evans (2000) except for the recently updated Franklin LIP mean (Denyszyn *et al.* 2009).

the same authors (Fanning & Link 2008). These dates strengthen the evidence for glaciogenic deposits in the Cordilleran rift basins that are younger than 700 Ma. Correlations across the Cordilleran margin of Laurentia have emphasized the close association of allegedly glaciogenic diamictites and volcanic rocks in that time frame. Evans (2000) suggested that all of these deposits could be correlative, with an age of *c.* 740–720 Ma. In that case, palaeomagnetic poles from the *c.* 720 Ma Franklin event could be used to infer palaeolatitudes of the Cordillera (applying the GAD field assumption and a rigid Laurentian plate). However, new data suggest some of the deposits of this diamictite–volcanic association are demonstrably younger, and therefore applications of the Franklin palaeomagnetic pole to undated Cordilleran deposits are tenuous. For these reasons, the Toby Formation's deep-tropical palaeolatitude estimate (Evans 2000) is no longer considered to be valid.

Elsewhere in western Laurentia, the Johnnie Rainstorm Member's incised canyons and features reminiscent of postglacial cap carbonates (Corsetti & Kaufman 2003) still retain the near-equatorial palaeolatitude of $01 \pm 4°$ as assessed by Evans (2000). Stratigraphically below that unit, but above the Kingston Peak glaciogenic unit, the Ibex Formation contains a polymictic conglomerate and overlying pink dolostone with negative carbon isotope values similar to many postglacial cap carbonates (Corsetti & Kaufman 2005). However, it is impossible to apply palaeomagnetic constraints from better dated units elsewhere in Laurentia without precise age constraints. A newly recognized glacial/cap-carbonate succession has been described in Sonora, Mexico (Corsetti *et al.* 2007), lacking both a precise age and a palaeomagnetic estimate of depositional palaeolatitude. Finally, although Evans (2000) included the Florida Mountains (New Mexico) diamictite

in his summary figure on glacial palaeolatitudes, that unit is demonstrably early Palaeozoic in age and is therefore excluded from the present analysis.

In the central Appalachians of eastern Laurentia, pebbly mudstone diamictites of the Grandfather Mountain Formation lie immediately above rhyolitic flows dated at 742 ± 2 Ma; this succession has been correlated with the Konnarock Formation diamictites and rhythmites with dropstones. In the Blue Ridge Mountains of Virginia, the *c.* 730–700 Ma Mechum River succession also contains glaciogenic features (Bailey *et al.* 2007). Evans (2000) correlated all three successions for the sake of simplicity, and estimated depositional palaeolatitudes based on a palaeomagnetic pole from the Franklin LIP at *c.* 720 Ma. In the present compilation, however, we distinguish the Grandfather Mountain and Konnarock formations from the Mechum River succession, based on slightly different ages as reviewed above. For the former units, we apply a new palaeomagnetic pole from the Kwagunt Formation in the Grand Canyon (Weil *et al.* 2004), which is precisely coeval at 742 ± 6 Ma (Karlstrom *et al.* 2000). Assuming negligible rotation of the Colorado Plateau relative to cratonic North America, as considered by Weil *et al.* (2004), this pole implies a palaeolatitude of $06 \pm 5°$ for the Konnarock/Grandfather Mountain region. Alternatively, a near-maximum estimate of Colorado Plateau rotation of 12° anticlockwise would imply a palaeolatitude for Konnarock/Grandfather Mountain at $04 \pm 5°$, within the error of the no-rotation model. This estimate is rated as only moderately reliable, because the dated Grandfather Mountain diamictites are not yet conclusively demonstrated as glacially influenced, and the presumed correlative Konnarock glaciogenic strata have more lax age constraints.

The Mechum River succession remains within the age range of the *c.* 720 Ma Franklin LIP, and the new grand-mean pole for that event (Denyszyn *et al.* 2009), implies a depositional palaeolatitude of $16 \pm 3°$ (assuming an internally rigid Laurentian plate and a geocentric axial dipole geomagnetic field). Stratigraphically higher in the succession, the Fauquier Formation contains a basal diamictite member, followed by a thick sandstone interval that is capped by a thin carbonate unit with a negative $\delta^{13}C$ excursion; in turn, this unit is followed conformably by basalts of the *c.* 570 Ma Catoctin Formation (Hebert *et al.* 2010). Palaeomagnetic results from the latter volcanic succession include two remanence components of greatly differing inclination, hence, implied palaeolatitude (Meert *et al.* 1994). The coexistence of both high- and low-inclination directions in these rocks is symptomatic of many broadly coeval igneous formations in eastern North America, leading to a fundamental debate on their general interpretation (e.g. Meert & Van der Voo 2001; Pisarevsky *et al.* 2001). The high-palaeolatitude Catoctin component is corroborated by other data of generally higher quality than the low-palaeolatitude data from the Iapetus margin of Laurentia (McCausland *et al.* 2007), so we prefer its implied palaeolatitude of $78 \pm 12°$ for the conformably underlying Fauquier Formation. This is the first near-polar estimate for a Neoproterozoic glacial deposit among recent palaeogeographic syntheses, but it is only somewhat reliable for the following reasons: (i) the Catoctin palaeomagnetic data remain ambiguous with respect to the two remanence components, (ii) the corroborating data from elsewhere in eastern Laurentia are also not of the highest quality, (iii) although the contact between the Fauquier Formation and the overlying basalts appears to be conformable, the basal Fauquier diamictites lie as much as hundreds of metres lower in the stratigraphy, and (iv) the 580–570 Ma interval appears to harbour very rapid apparent polar wander for Laurentia (McCausland *et al.* 2007), so absolute age uncertainties of only a few million years can permit a wide range of possible palaeolatitudes (tens of degrees) for sedimentary basins on that continent.

In Scotland and stratigraphically correlative areas of northern Ireland, the Port Askaig glaciogenic level is now generally correlated to the Sturtian ice ages (Prave 1999; Condon & Prave 2000;

McCay *et al.* 2006), but with the uncertainty surrounding the numerical age of Sturtian deposits, it is not possible to apply extra-basinal palaeomagnetic data to address the palaeolatitude of Port Askaig deposition. Older palaeomagnetic data obtained directly from the Port Askaig succession were summarized by Evans (2000) as unreliable, a conclusion followed here.

McCay *et al.* (2006) also identified a so-called Marinoan equivalent in northern Ireland, comprising the Stralinchy and Reelan Formations, based on the presence of diamictite, exotic clasts interpreted as dropstones, and a cap carbonate with a negative $\delta^{13}C$ anomaly. As with other putative Laurentian glaciogenic deposits of this age (assumed to be *c.* 635 Ma by correlation; see above), there are no available palaeomagnetic data from Laurentia that can be applied either directly from the relevant sedimentary basin or from elsewhere across the palaeocontinent.

The youngest purported Neoproterozoic glaciogenic unit in the Scottish and northern Irish Dalradian stratigraphic succession is the Loch na Cille boulder bed (and its correlative units). It closely overlies the Tayvallich Volcanics that have been recently re-dated at 601 ± 4 Ma (Dempster *et al.* 2002). The two relevant palaeomagnetic poles from Laurentia that approximate this age are from the Long Range dykes of Newfoundland and Labrador, dated by U–Pb at 615 ± 2 and $614 + 6/-4$ Ma (Kamo *et al.* 1989; Kamo & Gower 1994) and the Grenville Dykes of southeastern Ontario, dated at $590 + 2/-1$ Ma (Kamo *et al.* 1995). Both data sets contain an unusually large spread of inclinations and hence implied palaeolatitudes of emplacement, confounding simple interpretations (reviewed by Hodych & Cox 2007; McCausland *et al.* 2007). Low to moderate palaeolatitudes for the Long Range dykes (Murthy *et al.* 1992) are supported by subsequent work (McCausland *et al.* 2009, abstract only). For the younger, Grenville Dykes, a positive baked-contact test demonstrates that the steep palaeomagnetic B remanence found in some of the dykes is primary (Murthy 1971; Hyodo & Dunlop 1993). If these results withstand further scrutiny, then the Loch na Cille boulder bed would have been deposited during a migration of Laurentia from low to high latitudes.

For the East Greenland Neoproterozoic succession, Mac Niocaill *et al.* (2008) report in abstract some preliminary palaeomagnetic data that would appear to indicate rapid motion of Laurentia across palaeolatitudes. The upper Tillite Group glaciogenic unit bears a high-palaeolatitude magnetic remanence direction, but further sample analysis is needed to confirm that result.

Baltica

Several new geochronological and palaeomagnetic constraints have forced revision of Evans's (2000) estimate of depositional palaeolatitude of Neoproterozoic glaciogenic deposits on Baltica. First, the Vestertana Group, in which the palaeomagnetically studied Nyborg Formation lies between diamictite units of the underlying Smalfjord Formation and overlying Mortensnes Formation, has an imprecise palaeolatitude of $33 + 14/-12°$ (Torsvik *et al.* 1995). The reliability of this estimate has been downgraded because recent syntheses of Baltica's apparent polar wander path (Iglesia-Llanos *et al.* 2005) show the Nyborg pole to coincide with a *c.* 510 Ma overprint pole from elsewhere in Baltica. Because Middle Cambrian Finnmarkian deformation is prevalent in the northernmost Caledonides (Roberts 2003), there is a distinct possibility that the Nyborg palaeomagnetic remanence is an overprint acquired shortly before Finnmarkian folding, and thus not indicative of depositional palaeolatitudes. In addition, given the possibility of substantial age difference between the Smalfjord and Mortensnes Formations (e.g. correlations by Hoffman & Li 2009), the Nyborg pole is now considered as only applicable (if primary) to the conformably underlying Smalfjord Formation.

Elsewhere in Baltica, depositional palaeolatitudes on Ediacaran glacial deposits are similarly or even more poorly constrained. New ages exist for the Moelv diamictites of the southern

Norwegian sparagmite basins: younger than 620 ± 15 Ma detrital zircons in a distally underlying quartzite (Bingen *et al.* 2005) or perhaps even younger than 561 ± 4 Ma based on Re–Os dating of the immediately underlying Biri black shale (Hannah *et al.* 2007, abstract only). Nonetheless, the mid-Ediacaran apparent polar wander path for Baltica is highly uncertain (Iglesia-Llanos *et al.* 2005; Meert *et al.* 2007). Where Vilchitsy and Blon diamictite units are in close stratigraphic proximity to *c.* 551 Ma Volhyn volcanic rocks of the southwestern Baltic craton, palaeomagnetic results from the latter units imply a depositional palaeolatitude of $50 \pm 3°$ (A component of Nawrocki *et al.* 2004); however, nearly coeval sedimentary rocks of the White Sea region (555.3 ± 0.3 Ma; Martin *et al.* 2000) yield a more convincingly primary palaeomagnetic pole (Popov *et al.* 2002, 2005; Iglesia-Llanos *et al.* 2005) that implies a palaeolatitude of $28 \pm 3°$ for the Vilchitsy/Blon region. Any of these younger poles could also apply to the Moelv diamictite and correlative units in the Caledonides, now dated as late Ediacaran as noted above.

Ediacaran palaeogeography of Baltica is usually paired with eastern Laurentia, but both cratons' palaeomagnetic data appear to indicate rapid motions that challenge uniformitarian plate-tectonic interpretations (Abrajevitch & Van der Voo 2010; McCausland *et al.* 2011). Amid these uncertainties, the mid–late Ediacaran glacial palaeolatitudes of Baltica must be considered unresolved at present.

Altaids and Siberia

Chumakov (2009) has summarized the terminal Proterozoic to Cambrian stratigraphy across Kazakhstan and Kyrgyzstan, distinguishing between two prominent glacial levels (Satan, Rang, or Dzhetym Formations below, and Baykonur above). Both levels are younger than the *c.* 700 Ma volcanic complexes lying unconformably below. He also has described the Zabit Formation, in the East Sayan region, as glaciogenic and correlative with the Baykonur level, which is in turn correlated with the uppermost glacial level in Tarim (Hankalchough Formation; see below). A complex palaeomagnetic data set was obtained from the succession *c.* 1000 m or more above the Zabit diamictites into Cambrian strata (Kravchinsky *et al.* 2010), which may be useful for tectonic reconstructions but shed no direct light on glacial palaeolatitudes.

Two glaciogenic levels are also now recognized in the Dzhabkhan region of western Mongolia (Macdonald *et al.* 2009*b*): the basal, Maikhan Ul Member of the Tsagaan Oloom Formation, and the Khongoryn Member in the middle of the same formation. Chemostratigraphy of carbon isotopes in this succession supports correlation with the mid-Cryogenian (so-called Sturtian) and late Cryogenian (Marinoan) ice ages worldwide. Kravchinsky *et al.* (2001) found several components of magnetization through mainly the middle and upper parts of the Tsagaan Oloom Formation, and preferred a high-unblocking-temperature, low-palaeolatitude component as tentatively primary. That component, although of dual polarity, is not supported by field stability or reversals tests on the magnetization age, so is only somewhat reliable. Levashova *et al.* (2010) found a high-unblocking-temperature component of magnetization in the underlying Dzabkhan volcanic rocks, with U–Pb laser ablation ages of *c.* 800–770 Ma, with moderate palaeolatitudes of igneous emplacement. This estimate, however, would precede Maikhan Ul glaciogenic deposition by nearly 100 million years if the latter is correlated to the Rapitan ice age as discussed above (Macdonald *et al.* 2010*a*).

New recognition of late Neoproterozoic glaciation in southern Siberia has focused on the Yenisei ridge and the pre-Sayan region NW of Irkutsk. Sovetov (2002) and Sovetov & Komlev (2005) describe regional stratigraphic correlations around two distinct levels of diamictites with various glaciogenic features. The older Chivida unit of the Chingasan Group is more limited in geographic distribution in the Teya-Chapa trough (Yenisei region)

relative to the younger Pod'em Formation that is correlated to the Marnya Formation best exposed along the Biryusa and Uda Rivers (pre-Sayan). The Chivida diamictites are closely associated with volcanic rocks and are traditionally associated with an age of *c*. 700–750 Ma (Khomentovsky 1986), but they are not directly dated with modern methods. The Marnya Formation contains clasts that are speculated to derive from the Nersa Complex, a nearby mafic intrusive suite, according to Sovetov & Komlev (2005). Those authors quoted an Ar/Ar age of 611 ± 3 Ma for the Nersa Complex, but that age (now revised to 612 ± 6 Ma), in fact, derives from other mafic intrusive suites in southern Siberia (Gladkochub *et al.* 2006); thus the Marnya Formation diamictites lack any precise age constraints.

In the Patom region NE of Lake Baikal, at least two widespread glaciogenic levels have been reported: the older Kharlaktakh unit of the Ballaganakh Group and the younger Dzhemkukan or Bol'shoy Patom Formation of the Dal'nyaya Taiga Group (Pokrovskii *et al.* 2006; Sovetov 2008). No results from these successions are available in the global palaeomagnetic database.

The late Neoproterozoic to Early Cambrian palaeomagnetic apparent polar wander path for Siberia is highly contentious with a wide scatter of poles that universally imply low palaeolatitude for the craton; and if one includes the full range of data (Kirschvink & Rozanov 1984; Kravchinsky *et al.* 2001; Gallet *et al.* 2003; Metelkin *et al.* 2005) rather than a simplified selection (Cocks & Torsvik 2007), the problem is compounded further.

China cratons

Recent work has helped refine the chronology and palaeomagnetism of Neoproterozoic volcanic-sedimentary successions on the margin of the Tarim block in NW China. Two principal regions contain diamictites interpreted as glaciogenic deposits: Aksu in the west, and Quruqtagh in the east. The Aksu succession contains two diamictite levels, and a coarse magnetostratigraphic study by Li *et al.* (1991) yielded near-equatorial palaeolatitudes throughout the succession. More recently, Zhan *et al.* (2007) conducted a more detailed palaeomagnetic investigation of only the Sugetbrak Formation, which rests with disconformity upon the upper diamictite level (Yuermeinbrak Formation). Although Zhan *et al.* (2007) suggested that their high-stability, dual-polarity direction for the upper Aksu succession, which was acquired prior to folding of unspecified age, implies a palaeolatitude of *c*. 27° for the Yuermeinbrak ice age, there is lingering concern over why the palaeomagnetic results by Li *et al.* (1991) and Zhan *et al.* (2007), in part from the same sampling region on the same stratigraphic units, are so different. We tentatively accept the new constraint as more reliable, because the pole by Li *et al.* (1991) is similar to Cretaceous poles from Tarim and could represent an overprint of that age.

Farther east in the Tarim block, the Quruqtagh region contains three Neoproterozoic diamictite levels: Bayisi, Altungol-Tereeken and Hankalchough. The oldest level lies immediately above bimodal volcanic rocks dated by U–Pb SHRIMP at 740 ± 7 Ma (previously 755 ± 15 Ma from the same sample; Xu *et al.* 2005), and below volcanic rocks dated at 725 ± 10 Ma (Xu *et al.* 2009). The proximity of ages between volcanism and diamictite deposition allows the use of palaeomagnetic data from the former rocks (Huang *et al.* 2005) to constrain the latitude of glaciation, assuming the Bayisi diamictites are glaciogenic. That palaeomagnetic work found a characteristic remanence component of high consistency but no field tests were performed on its stability; it is therefore unclear whether its near-equatorial palaeolatitude $(01 + 4/-2°)$ is primary or secondary. It is rated here as only somewhat reliable. The Altungol-Tereeken diamictites, overlain by a notable pink cap carbonate, lie above the 725 Ma volcanic rocks and below another volcanic horizon dated at 615 ± 6 Ma (Xu *et al.* 2009). The Altungol-Tereeken interval has not been studied palaeomagnetically. In summary, both of the two recent

palaeomagnetic studies from Tarim demand further work to verify their applicability to Neoproterozoic glacial palaeolatitudes.

In the Qaidam terrane near the boundary between the Tarim and North China cratons, the Hongtiegou diamictite and overlying cap carbonate have been correlated, via stable isotope stratigraphy, to the uppermost Ediacaran (Sinian) successions in South China (Shen *et al.* 2010). Palaeomagnetic data are not available from the Neoproterozoic of Qaidam.

Chronology of the Sinian sedimentary basins in South China has improved vastly during the past few years. Two glacial levels are described with various local names, but generally referred to as the older Chang'an (or Tiesiao, or Jiangkou) episode and the younger Nantuo ice age. The Chang'an level is now bracketed in age between 725 ± 10 Ma (youngest U–Pb SHRIMP population from detrital zircons in the underlying Danzhou Group; Zhang *et al.* 2008) and 663 ± 4 Ma (Zhou *et al.* 2004). The Nantuo diamictite is younger than 654.5 ± 3.8 Ma and contains a basal tuff layer dated at 636.3 ± 4.9 Ma (Zhang *et al.* 2008), with a cap carbonate dated at 635.2 ± 0.6 Ma (Condon *et al.* 2005). Prior to the acquisition of these ages, Evans (2000) assigned a moderate depositional palaeolatitude to the Nantuo Formation based on results from the immediately underlying Liantuo redbeds (Evans *et al.* 2000). However, given that the Liantuo Formation contains an ash bed dated at 748 ± 12 Ma (Evans *et al.* 2000), the new dates from South China now preclude use of the Liantuo pole to constrain the significantly younger ice ages (Zhang *et al.* 2009).

Macouin *et al.* (2004) conducted a palaeomagnetic study on the Doushantuo Formation, which conformably overlies the Nantuo diamictites across most of South China. They obtained consistent results throughout the entire formation, implying near-equatorial palaeolatitudes, except for the postglacial cap carbonate at its base, which was palaeomagnetically unstable. Given that the Doushantuo Formation is now constrained to span more than 80 million years of time (Condon *et al.* 2005), and that the direction obtained by Macouin *et al.* (2004) is of single geomagnetic polarity, we suspect that it is a secondary overprint. The positive fold test only constrains the age of magnetization to pre-Mesozoic, and the direction is similar to both Early Cambrian and Silurian directions for South China. Zhang *et al.* (2009) correct numerous misconceptions about the stratigraphy and palaeomagnetic database for the Sinian of South China, and the best estimate for depositional palaeolatitude of the Nantuo diamictite reverts to the value obtained by Zhang & Piper (1997) from Yunnan Province, at $37 \pm 9°$. An identical result has been obtained by Zhang *et al.* (2006, abstract only) from Guizhou Province, supporting this conclusion. The soft-sediment fold test reported in the earlier study (Zhang & Piper 1997) imparts a high level of confidence to the moderate-palaeolatitude determination.

India to Nubia

Although Evans (2000) speculated that conglomerates within the Penganga Group might be glaciogenic, more thorough study of that region suggests no demonstrable glacial influence, as is evident, for example, in the discussions by Mukhopadhyay & Chaudhuri (2003) and Chakraborty *et al.* (2010). Other Neoproterozoic glaciogenic deposits in southern Asia are listed in Table 7.1.

In Iran, the so-called Infracambrian stratigraphic succession, between Neoproterozoic metamorphic basement and overlying nonmetamorphosed Cambrian sedimentary rocks, is variable in lithology but contains diamictite and lonestone-bearing units in its lower part, named the Rizu Formation (Huckriede *et al.* 1962; Hamdi 1992). The upper part of the succession is equally lithologically variable, as currently correlated across the country (Alsharhan & Nairn 1997), but contains rhyolites thought to be consanguineous with *c*. 530 Ma intrusions (Ramezani & Tucker 2003). No reliable palaeomagnetic data have yet been published on the Rizu strata or correlative rocks.

Despite a new, precise U–Pb TIMS age of 711.5 ± 1.1 Ma for the Ghubrah diamictite in the Jebel Akhdar region of northeastern Oman (Bowring *et al.* 2007; all sources of error included), its palaeolatitude remains poorly constrained. However, unmetamorphosed deposits of the possibly Ghubrah-correlative, lower Mirbat sandstone/diamictite assemblage, now renamed as the Ayn Formation (Rieu *et al.* 2006, 2007), yield a low-reliability palaeomagnetic direction (Kempf *et al.* 2000). This under-defined magnetization ($n = 10$ samples from two sites) would imply a palaeolatitude of $09 \pm 4°$ for the Ayn Formation, but we cannot include it in our final compilation due to the severely limited sample size.

On the younger and less precisely dated Fiq diamictite and its overlying Hadash cap carbonate, a two-polarity, pre-fold palaeomagnetic remanence implies a palaeolatitude of $13 \pm 7°$ for the Jebel Akhdar region, and $18 \pm 7°$ for the Mirbat region (Kilner *et al.* 2005), the latter area hosting the erosional remnants of an upper diamictite unit (Shareef Formation) that is correlated with the Fiq (Rieu *et al.* 2007). The folding is probably Palaeozoic in age, suggesting that the remanence could be primary. However, Rowan & Tait (2010, abstract only) have undertaken a more detailed magnetostratigraphic study of the Hadash cap carbonate in two sections with greatly differing structural attitudes, and have found the same remanence direction to be definitively post-folding, and possibly associated with regional remagnetization during emplacement of the Semail ophiolite. Given that only about 20% of the samples in the study by Kilner *et al.* (2005) yielded the preferred remanence direction, and only a few of their sites contributed significantly to their fold test, the low-palaeolatitude estimates for Fiq and Shareef diamictites can only be considered as somewhat reliable. Allen (2007) points out additional problems with the published data from Oman, in terms of their stratigraphic correlations and tectonic implications.

In the northern East African Orogen of Ethiopia, the Tambien Group contains a glaciogenic/cap-carbonate succession that has only recently been described in detail (Beyth *et al.* 2003; Miller *et al.* 2003). The Tambien Group is tightly folded into structures that are crosscut by the Mereb granite suite, dated by zircon Pb-evaporation on two plutons at 606.0 ± 0.9 and 613.4 ± 0.9 Ma (Miller *et al.* 2003), and by zircon U–Pb SHRIMP at 612.3 ± 7.5 Ma (Avigad *et al.* 2007). Detrital zircons in the Negash diamictite have yielded near-concordant U–Pb SHRIMP analyses as young as *c.* 750 Ma (Avigad *et al.* 2007; all younger diamictite detrital ages quoted in that work are more than 10% discordant). No palaeomagnetic data are available for the Tambien Group. Farther to the north in the Arabian–Nubian Shield, widespread banded Fe-formation is associated with diamictites of the Atud and Nuwaybah Formations (Stern *et al.* 2006; Ali *et al.* 2009).

Australia and Mawsonland

The palaeolatitude assessments by Evans (2000) remain valid for most of the many glaciogenic deposits scattered across the late Neoproterozoic glacial record of Australia. Ediacaran stratigraphic correlations in Australia are now under intense debate, following the recognition of the possibly glaciogenic Croles Hill Diamictite in Tasmania coincident with 582 ± 4 Ma rhyolite volcanism (Calver *et al.* 2004). Whether those diamictites correlate to the Elatina Formation in South Australia (by way of the Cottons Breccia on King Island), or whether they are substantially younger than Elatina, carries implications as profound as a factor-of-two uncertainty in the duration of the Ediacaran Period that begins, as formally defined, with deposition of the post-Elatina, Nuccaleena cap carbonate. No published palaeomagnetic data are available for the Tasmanian diamictites, but data are reported in abstract for the Cottons Breccia, with an implied palaeolatitude of $21 +9/-8°$; and the subsequent igneous activity dated at *c.* 580 Ma (Meffre *et al.* 2004), with implied palaeolatitudes

in the range of *c.* 12–21° (McWilliams & Schmidt 2003) that could be representative of Croles Hill deposition. As these data are reported in abstract only, they are omitted from our final compilation.

As for the Elatina glacial deposits and their continent-wide correlative units, new palaeomagnetic results add to an already long history of palaeomagnetic studies of this unit (reviewed by Evans 2000; Williams *et al.* 2008). Schmidt *et al.* (2009) presented a detailed analysis of palaeomagnetic data from both the Elatina and Nuccaleena formations in the Flinders Ranges, combining new results with previously published work. Based on moderate differences in remanent inclination between the two formations, they concluded that deglaciation coincided with rapid drift of the proto-Australian continent during a hiatus in deposition between the two units. The observed mean remanent inclination of 12.9° from the Elatina Formation would correspond to a depositional palaeolatitude of 6.5° if the geomagnetic field was dipolar and sedimentary inclination shallowing was negligible. For the Nuccaleena Formation, the mean inclination of 34.9° would correspond to a palaeolatitude of 19.2°. Schmidt *et al.* (2009) also reported results from four measurements designed to quantify the effects of remanence shallowing in the sedimentary rocks. In the first measurement, a correction for their measured values of remanence anisotropy would increase the Elatina inclination to 14.0°; however, Tauxe *et al.* (2008) showed that this method commonly underestimates the total amount of inclination shallowing. Indeed, two other measurements by Schmidt *et al.* (2009) appear to justify such an assessment. Their second test, elongation/inclination analysis on the distribution of data around the mean direction (using the assumed TK03 model of geomagnetic secular variation), would correct the Elatina inclination to 19° (bootstrap-generated uncertainties were not shown but are typically large for such tests). The third analysis, a dip test on crossbedded sandstones in the succession, would correct the Elatina inclination to between 18.4 and 20.2°. Because sandstones should be the least compacted of all the Elatina siliciclastic facies, this correction of the aggregate palaeomagnetic results include data from both sandstones and siltstones. The fourth test considered differences in inclination between carbonates and mudstones in the Nuccaleena Formation, the latter of which are expected to be more compacted than the former. The carbonates' mean inclination was 33.6° ($\alpha_{95} = 7.7°$), substantially greater than the mudstones' mean inclination of 21.1° ($\alpha_{95} = 7.8°$). Schmidt *et al.* (2009) claimed that these two means (taking into account both declination and inclination) were indistinguishable, using a test from McFadden & Lowes (1981). However, the test they used from that paper (equation 25) assumes an equivalency in concentration parameters between the two sample sets, which for the Nuccaleena data can be rejected with >99% confidence (Fisher *et al.* 1987, p. 219). If the correct test is used (the more general equation 23 from the same paper), the Nuccaleena data-derived statistic increases to 4.40, exceeding the $p = 0.05$ $F_{[2,76]}$ value of 3.12; thus, the carbonates' and mudstones' inclinations *are* significantly distinct at more than 95% confidence, and the Nuccaleena data therefore *do* support inclination shallowing having affected any fine-grained sedimentary rocks contributing to the mean directions in the sampling area (*contra* Schmidt *et al.* 2009).

In summary, the various inclination corrections to the Elatina palaeomagnetic data, as reported by Schmidt *et al.* (2009), imply a 'true' inclination value around 20°, with an implied palaeolatitude of approximately 10° for the sampled areas in the Flinders Ranges. Nuccaleena inclinations are steeper, due to the less-compacted carbonate lithology and perhaps also partly due to Australian plate motion between the ice age and the deglacial interval. Raub (2008) found a mean inclination of 27° ($\alpha_{95} = 3.5°$) for the Nuccaleena Formation, with several correlatable magnetozones spanning geodynamo reversals during deposition. That inclination value indicates a primary palaeolatitude of $14 \pm 2°$, between the estimates by Schmidt *et al.* (2009) for their compaction-corrected

Elatina and Nuccaleena data. Rare stratigraphic sections preserve sedimentological conformity (mixed transition) between siliciclastic rocks indistinguishable from Elatina Formation sandstones and Nuccaleena Formation cap-carbonate beds (Raub *et al.* 2007*a*), and the onlap relationships between the two formations described by Schmidt *et al.* (2009) can be accounted for by sediment draping of an irregular post-glacial topography, perhaps with diachronous onset of cap-carbonate deposition, without a substantial lacuna between the formations (Rose & Maloof 2010). For this reason, we propose that 10–14° of palaeolatitude best characterizes the Elatina/Nuccaleena glacial/postglacial palaeogeography. The 10–20° palaeolatitude range (as indicated in Fig. 7.1) also well represents the distribution of likely Elatina-correlative deposits across the Australian–Mawsonland palaeocontinent (Fig. 7.3). The compaction-corrected Elatina/Nuccaleena result is considered here to be one of the two most reliable palaeolatitude determinations among all Neoproterozoic glaciogenic deposits.

Grey *et al.* (2005) produced a landmark correlation of Neoproterozoic strata among deep boreholes throughout the Officer Basin of Western Australia, using diamictites and other indicators. New palaeomagnetic data from the Wahlgu diamictite level (correlated with the Elatina Formation) in the Lancer-1 borehole (Pisarevsky *et al.* 2007) generate a palaeolatitude of 7 ± 17°, but the data are highly scattered and merely consistent with the range of previous results from the Elatina Formation. Haines *et al.* (2008) revise the correlation of one diamictite and dropstone-bearing unit (therein named the Pirrilyungka Formation) to an age substantially older than the Wahlgu and Turkey Hill Formations, perhaps correlating with the Chambers Bluff diamictite in South Australia.

In the Kimberley region of northern Australia, the cap carbonate of the Walsh Tillite (western Kimberley) has yielded a moderate-palaeolatitude magnetic remanence supported by a tectonic fold test and two polarities of magnetization (Li 2000). Although the Walsh Tillite is variously correlated with either the Sturtian or Marinoan glacial level across Australia (see Corkeron 2007 for a summary), that issue is irrelevant for the reliability of the palaeomagnetic pole and its implications for deglaciation of the Walsh ice age. We accept the correlation by Corkeron & George (2001) of the Egan glaciogenic deposit (central Kimberley) with the Boonall dolomite in eastern Kimberley, and by further correlation using stromatolites, the mid-Ediacaran Julie Formation in central Australia. A palaeomagnetic pole from the latter region (Kirschvink 1978) implies a depositional palaeolatitude of 21 ± 8° for the Egan, assuming that the pole is primary and the correlations are correct.

Figure 7.3 shows two possible palaeogeographies of Australia during the time of terminal Cryogenian glaciation. The first representation (Fig. 7.3a) retains coherence of cratonic Australia in present-day coordinates, with palaeoequators according to the various palaeomagnetic studies of the Elatina or Nuccaleena formations. The second (Fig. 7.3b) incorporates a new model of Proterozoic Australia, with the northern part of the continent displaced from the western and southern parts by a local Euler rotation angle of 40° (Li & Evans 2011). In this model, the palaeoequator determined from the Walsh Tillite cap carbonate (Li 2000) returns to a position that is much closer to the palaeoequator attributed to the Nuccaleena cap carbonate in South Australia.

Southern Australia may also have been glaciated in the mid-Ediacaran interval. Gostin *et al.* (2011) describe possible ice-rafting features in the Bunyeroo Formation and equivalent units, which are demonstrated to have a pre-folding palaeomagnetic remanence that was acquired about 15° from the equator. In addition, Jenkins (2011) proposes a glacial influence on strata of the Billy Springs Formation higher in the stratigraphy.

Most tectonic syntheses of the region formerly known as East Gondwanaland now subdivide the cratonic areas of Antarctica into (at least) three fragments that collided during Cambrian time (e.g. Fitzsimons 2000). The Mawson Continent, or Mawsonland, comprises South Australia and adjacent regions of Antarctica in a pre-breakup Gondwanaland fit; those regions extend much of the length of the Transantarctic Mountains, from Victoria Land toward the South Pole. The Goldie Formation (redefined by Myrow *et al.* 2002) contains diamictites of uncertain depositional setting. Although no estimates of palaeolatitude are available from the Goldie Formation in the Transantarctic Mountains, its age is now tightly constrained by U–Pb on zircon, 668 ± 1 Ma, from interleaved mafic (meta)volcanic rocks (Goodge *et al.* 2002).

Kalahari and environs

Neoproterozoic glaciogenic deposits on the Kalahari craton are restricted to its present western margin, where as many as two diamictite levels are preserved in any single succession. In addition, several levels of canyon incision with diamictic infill are present within the Schwarzrand Subgroup of the Nama Group, spanning the Ediacaran–Cambrian boundary (reviewed by Evans 2000). No new palaeomagnetic constraints are available for any of the pre-Schwarzrand glacial levels, and the Schwarzrand palaeolatitude of 38 ± 3° (implied by the pole from the 547 ± 4 Ma Sinyai metadolerite on the Congo craton; Meert &
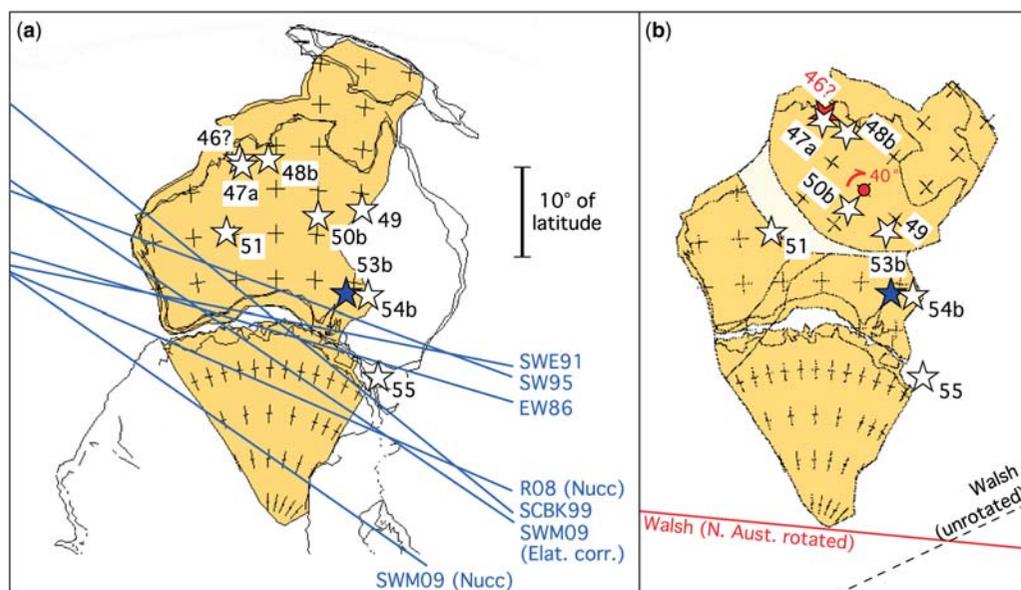

Fig. 7.3. (**a**) Palaeoequators plotted across Australia and Mawsonland, according to various palaeomagnetic studies of the Elatina Formation, or, as indicated, of the Nuccaleena Formation (Nucc). (**b**) Restoration of Ediacaran tectonic rotation between the northern and western/southern portions of cratonic Australia, following Li & Evans (2011). For star legend, see caption to Figure 7.2 (uncoloured stars representing deposits typically correlated with the Elatina glaciation. Palaeoequators are referenced as follows: EW86, Embleton & Williams (1986); SWE91, Schmidt *et al.* (1991); SW95, Schmidt & Williams (1995); SCBK, Sohl *et al.* (1999); R08, Raub (2008); SWM09, Schmidt *et al.* (2009); Walsh, Li (2000).

Van der Voo 1996) is assigned only low reliability because, despite excellent age constraints and the consistency of earliest Cambrian Gondwanaland palaeomagnetic poles from a variety of areas within the megacontinent (Mitchell *et al.* 2010), it remains unclear whether the Schwarzrand succession is truly glaciogenic.

Among older glaciogenic strata of the Gariep belt, Macdonald *et al.* (2010*c*) have revised correlations to distinguish two separate stratigraphic levels among outcrops previously lumped together as the Numees Formation. In this new correlation, the name 'Numees' is retained for an older level associated with an organic-rich cap carbonate typical of 'Sturtian' strata worldwide, whereas a new name, 'Namaskluft', is introduced for a younger level associated with a light-coloured peloidal cap carbonate typical of 'Marinoan' strata in other regions. Kaufman *et al.* (2009) review these successions and present an unconventional set of correlations with the global stratigraphic record, but it is not clear how such correlations might change according to the proposed distinction between Numees and Namaskluft glacial horizons. Farther south in the parautochthonous Gariep belt stratigraphy, the Aties Formation as listed by Evans (2000) has been subdivided into several new units, which include two glaciogenic levels recognized by Frimmel (2011): the lower Karoetjes Kop Formation, and the upper Bloupoort Formation. The former is correlated with the Kaigas diamictites in the Gariep belt to the north, whereas the latter is correlated to the Numees diamictites (s.l.), although further work is required to discern whether Bloupoort would correspond to Numees or Namaskluft, as distinguished by Macdonald *et al.* (2010*c*).

In the allochthonous Marmora terrane of the Gariep Belt, Namibia, diamictites and dropstone-bearing stratigraphic units are identified within the Dernburg Formation. These deposits are interpreted as having been deposited on a seamount in the Adamastor Ocean that lay between the Kalahari and Rio de la Plata cratons prior to their collision (Frimmel & Jiang 2001; Frimmel *et al.* 2002). No palaeomagnetic data are available for the Marmora terrane, although extensive carbonates and evaporites in the succession suggest low to moderate palaeolatitudes of deposition. Gaucher *et al.* (2009) included the Marmora terrane within a crustal block they named 'Arachania', inferred to have transferred from the Rio de la Plata craton to the Kalahari craton between *c.* 630 and 550 Ma.

Congo – São Francisco

The Katangan succession in east-central Africa contains two prominent diamictite horizons with overlying cap carbonates, named the Grand Conglomerat and Petit Conglomerat, in stratigraphic order. U–Pb SHRIMP ages of 765–735 Ma from volcanic strata, interbedded with diamictites that are correlated with the Grand Conglomerat (Key *et al.* 2001), overlap with a 748 ± 6 Ma date on the syenitic phase of the Mbozi complex from the same craton (Mbede *et al.* 2004, abstract only). This allows the Grand Conglomerat's depositional latitude to be estimated indirectly at 10 ± 5°, using the near-coeval Mbozi palaeomagnetic pole (Meert *et al.* 1995). This estimate is considered more reliable than the same pole applied for the Chuos Formation in northern Namibia, which might be substantially younger than the *c.* 750 Ma Mbozi pole. Both of these units are included separately in our new compilation because of the *c.* 1000 km lateral distance between their exposures, as well as the possibility that they are not precisely coeval. Our new estimate of Chuos depositional palaeolatitude differs slightly from that of Evans (2000) due to a refined location for the centre of Chuos-correlated strata in the northern and central Damara belt. As for the younger portion of these successions, there is still no reliable palaeomagnetic constraint on that unit, despite the recent U–Pb TIMS age constraint of 635.5 ± 1.2 Ma on a likely correlative of the Ghaub Formation in the internal sector of the Damara orogen (Hoffmann *et al.* 2004; but see also Kaufman *et al.* 2009).

Several recent papers provide additional insight on correlations of diamictite units across the present eastern and northern edges of the Congo–São Francisco craton. Melezhik *et al.* (2006) provide stable isotopic data bearing on regional and global stratigraphic correlations of the Geci metacarbonates in northern Mozambique, which are associated with metadiamictites that may be glaciogenic (Pinna *et al.* 1993). To the NW, Poidevin (2007) reviews stratigraphic data from the Oubanguide belt in central Africa, whereas Caron *et al.* (2010) report the discovery of a new diamictite cap-carbonate succession in southern Cameroon. Lack of precise ages on all of these units, as well as a general dearth of late Neoproterozoic palaeomagnetic data from the Congo craton, prohibit assignment of depositional palaeolatitudes.

Continuing around the São Francisco side of the craton, in Brazil, the various lithostratigraphic names for late Neoproterozoic diamictites are well summarized by Misi *et al.* (2007) and Sial *et al.* (2009). As many as two or perhaps three glaciogenic levels are known from each area, with few precise age constraints and thus, many possible correlations across the region (see also Kaufman *et al.* 2009). A comprehensive summary of all these possible relationships is beyond the scope of the present paper, but Table 7.1 splits the deposits into many distinct geographical and tectonostratigraphic subdivisions, which later can be combined as correlations gain reliability. In the cratonic autochthon, the basal Bambuí cap carbonate (Sete Lagoas Formation) has yielded a Pb/Pb isochron age of 740 ± 22 Ma (Babinski *et al.* 2007), and the authors of that study infer a depositional palaeolatitude according to *c.* 750 Ma palaeomagnetic data from Africa; however, we consider the Sete Lagoas age constraints lax enough to render its palaeolatitude assignment too tentative. Another age constraint of particular note is an astounding Re–Os black shale isochron in the 1100–1000 Ma range (Azmy *et al.* 2008) for the Lapa Formation (uppermost formation in the diamictite-bearing Vazante Group) that, if correct, would represent the first discovery of a Mesoproterozoic ice age, anywhere in the world. However, Rodrigues *et al.* (2008, extended abstract) find <1000 Ma detrital zircons in all Vazante units, in direct contrast to the Re–Os ages. As for palaeomagnetic constraints, the Salitre cap carbonate of the Bebedouro Formation has only yielded a Cambrian remagnetization (Trindade *et al.* 2004). No reliable palaeomagnetic data are available for the other diamictites of the São Francisco craton.

West Africa and Hoggar

Although Evans (2000), following earlier syntheses across the Taoudeni basin, considered the possibility that the glaciogenic 'triad' succession is late Ediacaran to earliest Cambrian in age, a more detailed study of that succession in the Volta basin (Porter *et al.* 2004) provides compelling chemostratigraphic comparisons with basal Ediacaran cap carbonates elsewhere in the world that are dated at 635 Ma (South China and Namibia, see above). Further, the assigned Early Cambrian age of the glaciogenic Hassanah Diallo Formation in Senegal, based on a small shelly fossil assemblage in dolomite resembling cap carbonate, is now retracted with the interpretation that the fossiliferous sample was collected from a loose boulder fallen from overlying strata (Shields *et al.* 2007). For these reasons, the indirect estimation of triad palaeolatitudes from an Early Cambrian aggregate Gondwana Land apparent polar wander path (Evans, 2000) now appears inappropriate. As discussed in Evans (2000), previous palaeomagnetic data from the Taoudeni sedimentary succession are of questionable reliability. However, a new result from one site of the 'triad' cap carbonate in the Gourma region indicates a magnetic remanence that was acquired prior to Pan-African folding in the area (Boudzoumou *et al.* 2011). If primary, the result would imply a depositional palaeolatitude of 08 ± 7°, but because of the small sample size, the result warrants further study before it can be considered as reliable as the other determinations shown in Figure 7.1.

Alleged periglacial features from the base of the Atar Group (Trompette 1994), which were discussed by Evans (2000) with additional references, must now be considered as Mesoproterozoic, given multi-sample, black shale Re–Os isochron ages of c. 1105 Ma (Rooney et al. 2010) from somewhat higher levels in the succession. The ages are reminiscent of those from the Vazante Group and its diamictites, marginal to the São Francisco craton (see above), but the Atar Re–Os isochrons have lower mean square of weighted deviates values and thus, are more reliable. The alleged periglacial influence on the basal Atar sediments should be tested by further study.

Despite new U–Pb ages from the Anti-Atlas Mountains of Morocco, late Neoproterozoic glaciogenic deposits there remain unconstrained in depositional palaeolatitude. The older Sarhro diamictites in the Sirwa region were deformed and metamorphosed c. 660 Ma (Thomas et al. 2002, 2004). Although Thomas et al. (2004) advocate the traditional correlation of the Sarhro Group with the Tiddiline succession in the Bou Azzer–El Graara inlier, the latter diamictite-bearing succession contains boulder-sized clasts of the Bleïda granodiorite now dated at 579.4 ± 1.2 Ma (Inglis et al. 2004). Therefore, the new stratigraphic constraints appear to distinguish the two successions in age by c. 100 million years. No reliable palaeomagnetic data exist for the older age interval, but the Tiddiline succession depositional palaeolatitude could be estimated by the immediately overlying, and penecontemporaneous (c. 575–560 Ma; Thomas et al. 2002; Maloof et al. 2005), Ouarzazate volcanic group. Unfortunately, the existing palaeomagnetic results from those rocks are of near-zero reliability, as summarized by Tohver et al. (2006).

Avalonia and Cadomia

The Gaskiers glaciation is now dated by U–Pb TIMS to c. 580 Ma (Bowring et al. 2002, abstract only), and serendipitously, the age of the Marystown volcanic rocks (used by Evans 2000 to estimate Gaskiers depositional palaeolatitudes) has also been revised to c. 585–575 Ma (McNamara et al. 2001). The concordance of these ages increases the likelihood that the Marystown palaeolatitude of $34 + 8/-7°$ applies to the Gaskiers deposit. It is considered here as only moderately reliable as an indicator for global palaeoclimate models, because the Gaskiers unit is geographically limited and of short-lived duration (Bowring et al. 2002), and thus, it may represent only local, alpine glaciation in an active-margin tectonic setting.

In the Boston basin, the Roxbury Conglomerate has yielded a magnetization in nonglacial red slates bracketing the glaciogenic Squantum Member, which is consistent with that of unconformably underlying volcanic rocks, and partially supported by a positive conglomerate test on those volcanic rocks (Fang et al. 1986). Further palaeomagnetism and geochronology of this same succession (Thompson et al. 2007) has found that the c. 600–595 Ma, pre-Squantum, Mattapan volcanic rocks yielded a distinct magnetization that had not been recovered previously, and the earlier characteristic magnetization of Fang et al. (1986) was not reproduced. Thompson et al. (2007) reported a possibly primary component from only one site of the Squantum unit, and did not discuss the discrepancy between their results and those of the earlier study. Because the Squantum Member is younger than 593 Ma (U–Pb on detrital zircons; Thompson & Bowring 2000) but otherwise poorly constrained in age, it is possible that the difference is due to plate motions and rotations of the Avalonian arc, between deposition of the volcanic rocks and the overlying glaciogenic succession. We continue to use the directly obtained result of Fang et al. (1986) in our analysis, implying a depositional palaeolatitude of $55 + 8/-7°$.

In the Anglesey region of Wales, an East Avalonian accretionary 'Mona' complex includes heterolithic, cobble-supporting, volcaniclastic mudstone (Gwna Group) of interpreted ophiolitic affinity, plausibly representing ice-rafted debris of Gaskiers-correlative age in an open ocean setting between 595 and 550 Ma (Kawai et al. 2008). The authors of the study inferred a moderate depositional palaeolatitude from the presumably adjacent Avalonian arc: the 580–575 Ma Marystown Volcanics (see above) and the c. 603 Ma Caldecote Volcanics plus related intrusions (Vizan et al. 2003). We suspect that this estimate is unreliable, given the combined uncertainties in glacial influence of the Gwna beds, palaeogeographic affinity of the Mona complex relative to the Avalonian arc, and age of the succession.

In the Cadomian terrane, Bohemian massif, marine diamictite lenses associated with inferred, glacially influenced, base level changes are found in the Clanzschwitz and Weesenstein Groups. These lenses contain detrital zircons as young as c. 570 Ma, and therefore, their deposition is also approximately the same age (Linnemann et al. 2007). These formations, in the Saxo-Thuringian Zone, were likely proximal to West Africa during Ediacaran to early Palaeozoic time; however, lack of reliable Ediacaran palaeomagnetic data from either the Cadomian Belt itself or the West African craton prohibit assignment of depositional palaeolatitudes for the Clanzschwitz and Weesenstein units.

Amazonia and environs

In the Paraguay belt at the southeastern margin of the Amazon craton, the Puga diamictite is overlain by the Mirassol d'Oeste cap carbonate. A characteristic component of magnetization has been found in the cap dolostone (Trindade et al. 2003), carried by both magnetite and haematite with high rock-magnetic stability (Font et al. 2005) and multiple reversals were observed through the stratigraphic section (Font et al. 2010) exposed in a single rock quarry. If primary, that magnetic remanence would indicate a depositional palaeolatitude of $22 + 6/-5°$ for Puga deglaciation. The direction, however, is coincident with the Mesozoic to recent expected directions at the sampling sites. Although the presence of two magnetic polarities is encouraging, remagnetizations of that nature are well known in the palaeomagnetic literature (e.g. Kent & Dupuis 2003), and the Mirassol d'Oeste characteristic remanence is so far observed at only a single sampling locality with no field stability tests on its age. For this reason, it is considered here to be only moderately reliable.

Higher in the stratigraphy, the Serra Azul Formation is now recognized as a second glaciogenic level in the Paraguay belt (summarized by Alvarenga et al. 2009). Age constraints are lax, and its depositional palaeolatitude is unknown.

Along coastal Peru, the Arequipa massif contains a diamictite unit, the Chiquerío Formation, which has been correlated to glaciogenic deposits in eastern Laurentia (see references in Evans 2000). Recent U–Pb dating of its host terrane, the Arequipa-Antofalla block (AAB), however, has identified more compelling tectonic affinities to the Amazon craton (Chew et al. 2007; Casquet et al. 2010). In either case, without a precise age, the Chiquerío diamictite's depositional palaeolatitude remains unconstrained.

Rio de la Plata craton and environs

The Las Ventanas and Playa Hermosa Formations, near the eastern edge of the Rio de la Plata craton in southern Uruguay, contain the most convincingly glaciogenic features in the entire region (Pazos et al. 2003, 2008; Pecoits et al. 2008). Their age constraints are not well defined within the Ediacaran Period. Palaeomagnetic results obtained directly from the Playa Hermosa Formation suggest a tropical palaeolatitude of $13 + 9/-8°$ (Sánchez-Bettucci & Rapalini 2002), but we exclude this result from our final analysis because of very limited sampling in that preliminary study.

Lower in the stratigraphy, within the same tectonic unit (Nico Pérez terrane and adjacent portion of the Dom Feliciano belt), the Zanja del Tigre Formation is reported to contain a thin metadiamictite horizon as part of a succession (Lavalleja Group) that

metamorphosed at *c.* 630 Ma (Pazos *et al.* 2008, fig. 4). A glacio-genic influence is disputed for these metamorphic rocks (Gaucher & Poiré 2009; Pecoits & Aubet, pers. comm. 2009) and, regardless, depositional palaeolatitudes for this unit are unconstrained.

Within the southern Brazilian portion of the Dom Feliciano belt, Eerola (2006) identified isolated cobbles within schists of the Brusque Group, which he correlated with the *c.* 750 Ma Chuos Formation in Namibia. However, a much older age for the Brusque succession is possible, as it contains no detrital zircons younger than 2000 Ma (Hartmann *et al.* 2003). A glaciogenic origin for this unit is not yet well demonstrated, but interestingly, Pazos *et al.* (2008) suggest correlation of the Brusque Group with the Lavalleja Group. This correlation suggests that scattered remnants of a pre-630 Ma ice age could be present throughout the region. However, the name Lavalleja Group has been applied to various metamorphic rocks with protolith ages now found to range from Archaean to Ediacaran (Bossi & Cingolani 2009); thus, all correlations should be treated with caution.

Eerola (1995) also described diamictites and dropstone-bearing laminated mudstones in the Camaquã basin, referred to as the Passo da Areia Formation (see also Pazos *et al.* 2008) or, alternatively, the Picada das Graças Formation (Eerola 2006; Janikian *et al.* 2008). Any proposed glacial influence for that unit was discounted by the latter study (Janikian *et al.* 2008), which provided a direct U–Pb SHRIMP zircon age of 580.0 ± 3.6 Ma from an interbedded tuff. Janikian *et al.* (2008) cite a palaeolatitude of $23 + 10/-7°$ from the slightly older Hilario Formation volcanic rocks, but as reviewed by Tohver *et al.* (2006), that study lacks field tests and is only of moderate reliability. Nonetheless, farther north in the Ribeira belt, Campanha *et al.* (2008) have determined a maximum age limit of *c.* 590–580 Ma for diamictites of the highly deformed Iporanga Formation, which contain exotic clasts and thus, could be of glaciogenic origin. Given the more convincing glacial influence on the Las Ventanas and Playa Hermosa formations of the same general age range on the proximal Rio de la Plata craton, the Iporanga strata should be investigated further to confirm or refute the influence of ice during sedimentation.

Trindade & Macouin (2007) refer to glaciation at moderate to high palaeolatitudes in the Rio de la Plata craton, constrained by the 'La Tinta' palaeomagnetic pole (see below), and depicted as such in a 620 Ma global reconstruction. That citation probably refers to the Sierra del Volcán Formation, recognized as bearing glaciogenic features with a possible Sturtian age (Pazos *et al.* 2003). However, the unit lacks precise geochronological data (Pazos *et al.* 2008) and in fact could be as young as Ordovician (unpublished detrital zircon ages cited by Poiré & Gaucher 2009). Regardless, the La Tinta pole is now considered to represent a probable Cambrian overprint (Rapalini & Sánchez-Bettucci 2008), leaving these deposits completely unconstrained in depositional palaeolatitude.

Discussion

Figure 7.1 summarizes the results of our updated synthesis. Although several of the assessments of glacial palaeolatitudes have changed in detail, owing to new geochronologic or palaeomagnetic data, the general result is essentially the same as that determined by Evans (2000): low and moderate palaeolatitudes are abundant, at all reliability levels, whereas few if any near-polar ($>60°$) glacial deposits have thus far been identified in the Neoproterozoic rock record. From a total of 137 stratigraphic units distinguished in the present analysis, only 22 deposits have depositional palaeolatitude constraints that are at least 'somewhat' reliable, and among these, merely 10 are constrained moderately well. Only three deposits (Upper Tindir, Nantuo and Elatina) are considered to have the highest degree of reliability, and all were laid down in low to moderate palaeolatitudes. The lowest of these, Elatina, is supported by numerous field stability tests to

verify the primary age of magnetization; reproducibility by four different palaeomagnetic laboratories through 15 years of study; and several independent, quantitative methods to correct for modest amounts of sedimentary inclination shallowing. Several lines of evidence demonstrate the effects of regionally cold climates near sea level during the Elatina ice age (Williams *et al.* 2008). The conclusion appears inescapable: Neoproterozoic continental ice sheets extended deep within the tropics.

Among the other high- to moderate-reliability data shown in Figure 7.1, the only other results obtained from sedimentary rocks are the Puga, Nantuo and Walsh. Puga and Walsh magnetizations are dominated by carbonate-associated haematite, so these results also may be less prone to inclination bias. The Nantuo result represents siliciclastic rocks, so its remanence could be slightly shallowed in inclination and hence, shallowed in palaeolatitude. However, estimates for the Konnarock, Rapitan, Mechum River, Grand Conglomerat, Upper Tindir and Gaskiers deposits are calculated indirectly from coeval igneous rocks on the same cratons. Those results are not affected by inclination shallowing.

Concerns that the Neoproterozoic geomagnetic field was either nonaxial or nondipolar are valid in principle, but many palaeomagnetic results, including those from the Elatina-Nuccaleena succession, show typical patterns of a sporadically reversing field with circularly symmetric secular variation about the time-averaged mean (e.g. Raub 2008; Schmidt *et al.* 2009; Font *et al.* 2010). It should therefore be emphasized that a non-actualistic geodynamo invoked to produce strictly polar or temperate glacial palaeolatitudes from the available palaeomagnetic database is as shockingly nonuniformitarian to geophysicists as near-equatorial glaciation is to palaeoclimatologists. Similarly, hypotheses invoking rapid palaeolatitude shifts of continents to generate erroneous palaeomagnetic latitudes, due to lax age constraints in some instances, would require such motions at rates beyond what is normally considered reasonable for plate tectonics. Such shifts would need to be consistently biased to produce wholly low- to mid-palaeolatitudes at the expense of any polar results.

Evans (2006) showed that Proterozoic evaporites produce subtropical palaeomagnetic latitudes, as expected for a uniformitarian geodynamo, as well as low planetary obliquity. Williams (2008) attempted to discredit the latter conclusion by appealing to uncertainties in geomagnetic polarity, to generate an equatorial mean for the evaporites, as predicted by numerical simulations of high-obliquity palaeoclimate. However, that issue was already foreseen and refuted by Evans (2006), who wrote (p. 53) 'A zero mean could be obtained if half of the palaeolatitudes were considered to represent the opposite hemisphere (geomagnetic polarity being generally unknown in the Precambrian), but even then the total distribution would be significantly bimodal, in contrast with the high-obliquity model predictions.'

Our summary analysis (Fig. 7.1) differs from the similar figure in Evans (2000) in several minor ways; most importantly (i) a slight increase in the estimated depositional palaeolatitude of the Rapitan deposits, based on new geochronology that allows precise application of the higher-reliability Franklin large igneous province pole that is immune to sedimentary inclination shallowing, (ii) a slight increase in the estimated depositional palaeolatitude of the Elatina deposits, based on new studies that quantify such inclination shallowing by several independent methods, (iii) exclusion of the Jbeliat palaeolatitude estimate due to its more conclusively pre-Cambrian age and thus inappropriateness of applying Early Cambrian palaeolatitudes from the Gondwana Land apparent polar wander path, and (iv) inclusion of the somewhat reliable, near-polar palaeolatitude for the Fauquier Formation as determined by palaeomagnetism on the overlying Catoctin basalts and related intrusions. This last entry needs to be confirmed, but if so, it has the potential to strike down a pillar of the Precambrian high-obliquity Earth model (Williams 1993, 2008) – that Precambrian glaciogenic deposits are only known from the palaeo-tropics, rather than the palaeo-poles. In general,

however, our update does not significantly affect the basic conclusion by Evans (2000) of a preponderance of low- to mid-latitudes for Neoproterozoic glaciation.

Our analysis is the most detailed of its kind in the published literature. Although our conclusions are nearly opposite to those of Eyles & Januszczak (2004), we note that their analysis included less than a fifth of the number of deposits considered herein. Among the deposits accepted by them as having 'demonstrated' glacial influence, five have palaeolatitudes of at least somewhat reliable quality ranging between 13 and 37°. One of the deposits (Rapitan) has moderate palaeomagnetic reliability indicating tropical palaeolatitudes. Although we did not assess the evidence for or against glacial influence on sedimentation in our present analysis, we anticipate that future efforts in that regard will consider the full extent of units listed in Table 7.1.

Trindade & Macouin (2007) also considered only a small fraction of the deposits listed in Table 7.1, although their conclusion is similar to ours. Considering only the subset of deposits discussed by Trindade & Macouin (2007), the most striking differences between their conclusions and ours are as follows: (i) our exclusion of the Scout Mountain palaeolatitude based on an updated age for that unit, which differs from the palaeomagnetically studied rock units elsewhere in Laurentia, (ii) our inclusion of a Gaskiers palaeolatitude applied indirectly from a palaeomagnetic study of precisely coeval igneous rocks in Avalon, (iii) our estimate of mid-latitude deposition for the Nantuo ice age, rather than near-equatorial, based on our selection of the direct Nantuo constraint, rather than the (in our opinion) lower-reliability Doushantuo result, and (iv) our estimate of low-latitude deposition of the Playa Hermosa Formation, preferred over the higher latitudes implied by the now-obsolete La Tinta Formation.

The most interesting comparison to earlier palaeogeographic syntheses is between our present analysis and that of Hoffman & Li (2009). The essence of our conclusions is similar: only low- and mid-latitudes have been moderately or highly reliably determined for most Neoproterozoic glacial deposits. The principal exception to this rule stems from Ediacaran deposits such as Loch na Cille, Squantum, Gaskiers and Serra Azul, all of which are estimated at >60° palaeolatitude by Hoffman & Li (2009). Among those units, we only consider Squantum and Gaskiers as having direct palaeomagnetic constraints classified as even somewhat reliable, and the Gaskiers palaeolatitude, by our estimation, is remarkably different at $31 + 10/-8°$. These discrepancies can be attributed to the very distinct approaches between the two studies. We took a bottom-up approach that considered ages and palaeolatitudes unconstrained unless demanded by strictly relevant data, whereas Hoffman & Li (2009) adopted a top-down approach that assumed known glacial ages within a specified global plate-kinematic model. That model was based on a mostly independent palaeomagnetic database obtained primarily from well-dated igneous rocks with little relationship to glacial units. So, although both studies derive from the palaeomagnetic method, they are quite distinct in the assumptions and selection of data. The principal discordance between our work and that of Hoffman & Li (2009) occurs during the mid-Ediacaran interval, when the global palaeogeographic models are most uncertain. This period is associated with the fastest continental motions in Earth history, which may be attributed, in part, to global tectonic reorganization (Hoffman 1999), rapid true polar wander (Raub et al. 2007b) and an isolated episode of nonuniformitarian geodynamo behaviour (Abrajevitch & Van der Voo 2010). If such an isolated episode occurred, and it is far from proven, then it would appear to be limited to the mid-Ediacaran interval rather than the late Cryogenian, Elatina or Puga ice ages (with uniformitarian symmetry in two-polarity palaeomagnetic directions), or the older Cryogenian, Upper Tindir/Rapitan ice age (as judged by the highly stable Franklin palaeomagnetic pole).

In summary, the palaeomagnetic case for low-latitude Neoproterozoic glaciation is strong, and Snowball Earth remains an attractive model for evaluating the enigmatic geological record of icehouse and hothouse environmental conditions just prior to the dawn of animal life on our planet.

References

ABRAJEVITCH, A. & VAN DER VOO, R. 2010. Incompatible Ediacaran paleomagnetic directions suggest an equatorial geomagnetic dipole hypothesis. *Earth and Planetary Science Letters*, **293**, 164–170.

ALI, K. A., STERN, R. J., MANTON, W. I., JOHNSON, P. R. & MUKHERJEE, S. K. 2009. Neoproterozoic diamictite in the Eastern Desert of Egypt and Northern Saudi Arabia: evidence of ∼750 Ma glaciation in the Arabian–Nubian Shield? *International Journal of Earth Sciences*, doi: 10.1007/s00531-009-0427-3.

ALLEN, P. A. 2007. The Huqf Supergroup of Oman: basin development and context for Neoproterozoic glaciation. *Earth-Science Reviews*, **84**, 139–185.

ALLEN, P. A. & ETIENNE, J. L. 2008. Sedimentary challenge to Snowball Earth. *Nature Geoscience*, **1**, 817–825.

ALSHARHAN, A. S. & NAIRN, A. E. M. 1997. Chapter 3: Infracambrian of the Middle East. *In*: ALSHARHAN, A. S. & NAIRN, A. E. M. (eds) *Sedimentary Basins and Petroleum Geology of the Middle East*. Elsevier, Amsterdam, 65–86.

ALVARENGA, C. J. S. de, BOGGIANI, P. C., BABINSKI, M., DARDENNE, M. A., FIGUEIREDO, M., SANTOS, R. V. & DANTAS, E. L. 2009. The Amazonian palaeocontinent. *In*: GAUCHER, C., SIAL, A. N., HALVERSON, G. P. & FRIMMEL, H. E. (eds) *Neoproterozoic–Cambrian Tectonics, Global Change and Evolution*. Elsevier, Amsterdam, Developments in Precambrian Geology, **16**, 15–28.

AVIGAD, D., STERN, R. J., BEYTH, M., MILLER, N. & MCWILLIAMS, M. O. 2007. Detrital zircon U–Pb geochronology of Cryogenian diamictites and Lower Paleozoic sandstone in Ethiopia (Tigrai): age constraints on Neoproterozoic glaciation and crustal evolution of the southern Arabian–Nubian Shield. *Precambrian Research*, **154**, 88–106.

AZMY, K., KENDALL, B., CREASER, R. A., HEAMAN, L. & DE OLIVEIRA, T. F. 2008. Global correlation of the Vazante Group, São Francisco Basin, Brazil: Re–Os and U–Pb radiometric age constraints. *Precambrian Research*, **164**, 160–172.

BABINSKI, M., VIEIRA, L. C. & TRINDADE, R. I. F. 2007. Direct dating of the Sete Lagoas cap carbonate (Bambuí Group, Brazil) and implications for the Neoproterozoic glacial events. *Terra Nova*, **19**, 401–406.

BAILEY, C. M., PETERS, S. E., MORTON, J. & SHOTWELL, N. L. 2007. The Mechum River Formation, Virginia Blue Ridge: a record of Neoproterozoic and Paleozoic tectonics in southeastern Laurentia. *American Journal of Science*, **307**, 1–22.

BEYTH, M., AVIGOD, D., WETZEL, H.-U., MATTHEWS, A. & BERHE, S. M. 2003. Crustal exhumation and indications for Snowball Earth in the East African Orogen: north Ethiopia and east Eritrea. *Precambrian Research*, **123**, 187–201.

BINGEN, B., GRIFFIN, W. L., TORSVIK, T. H. & SAEED, A. 2005. Timing of Late Neoproterozoic glaciation on Baltica constrained by detrital zircon geochronology in the Hedmark Group, south-east Norway. *Terra Nova*, **17**, 250–258.

BOSSI, J. & CINGOLANI, C. 2009. Extension and general evolution of the Río de la Plata Craton. *In*: GAUCHER, C., SIAL, A. N., HALVERSON, G. P. & FRIMMEL, H. E. (eds) *Neoproterozoic–Cambrian Tectonics, Global Change and Evolution*. Elsevier, Amsterdam, Developments in Precambrian Geology, **16**, 73–85.

BOUDZOUMOU, F., VANDAMME, D., AFFATON, P. & GATTACCECA, J. 2011. Neoproterozoic paleomagnetic poles in the Taoudeni basin (West Africa). *Comptes Rendus Geoscience*, **343**, 284–294.

BOWRING, S. A., LANDING, E., MYROW, P. & RAMEZANI, J. 2002. Abstract #13045-Geochronological constraints on terminal Neoproterozoic events and the rise of metazoans. *Astrobiology*, **2**, 457–458.

BOWRING, S. A., GROTZINGER, J. P., CONDON, D. J., RAMEZANI, J., NEWALL, M. J. & ALLEN, P. A. 2007. Geochronologic constraints on the chronostratigraphic framework of the Neoproterozoic Huqf Supergroup, Sultanate of Oman. *American Journal of Science*, **307**, 1097–1145.

CALVER, C. R., BLACK, L. P., EVERARD, J. L. & SEYMOUR, D. B. 2004. U–Pb zircon age constraints on late Neoproterozoic glaciation in Tasmania. *Geology*, **32**, 893–896.

CAMPANHA, G. A. C., BASEI, M. S., TASSINARI, C. C. G., NUTMAN, A. P. & FALEIROS, F. M. 2008. Constraining the age of the Iporanga Formation with SHRIMP U–Pb zircon: implications for possible Ediacaran glaciation in the Ribeira Belt, SE Brazil. *Gondwana Research*, **13**, 117–125.

CARON, V., EKOMANE, E., MAHIEUX, G., MOUSSANGO, P. & NDJENG, E. 2010. The Mintom Formation (new): sedimentology and geochemistry of a Neoproterozoic, Paralic succession in south-east Cameroon. *Journal of African Earth Sciences*, **57**, 367–385.

CASQUET, C., FANNING, C. M., GALINDO, C., PANKHURST, R. J., RAPELA, C. W. & TORRES, P. 2010. The Arequipa Massif of Peru: new SHRIMP and isotope constraints on a Paleoproterozoic inlier in the Grenvillian orogen. *Journal of South American Earth Sciences*, **29**, 128–142.

CHAKRABORTY, P. P., DEY, S. & MOHANTY, S. P. 2010. Proterozoic platform sequences of Peninsular India: implications towards basin evolution and supercontinent assembly. *Journal of Asian Earth Sciences*, **39**, 589–607.

CHEW, D., KIRKLAND, C., SCHALTEGGER, U. & GOODHUE, R. 2007. Neoproterozoic glaciation in the Proto-Andes: tectonic implications and global correlation. *Geology*, **35**, 1095–1098.

CHUMAKOV, N. M. 2009. The Baykonurian glaciohorizon of the Late Vendian. *Stratigraphy and Geological Correlation*, **17**, 373–381.

COCKS, L. R. M. & TORSVIK, T. H. 2007. Siberia, the wandering northern terrane, and its changing geography through the Palaeozoic. *Earth-Science Reviews*, **82**, 29–74.

CONDON, D. J. & PRAVE, A. R. 2000. Two from Donegal: Neoproterozoic glacial episodes on the northeast margin of Laurentia. *Geology*, **28**, 951–954.

CONDON, D., ZHU, M., BOWRING, S., WANG, W., YANG, A. & JIN, Y. 2005. U–Pb ages from the Neoproterozoic Doushantuo Formation, China. *Science*, **308**, 95–98.

CORKERON, M. 2007. 'Cap carbonates' and Neoproterozoic glacigenic successions from the Kimberley region, north-west Australia. *Sedimentology*, **54**, 871–903.

CORKERON, M. L. & GEORGE, A. D. 2001. Glacial incursion on a Neoproterozoic carbonate platform in the Kimberley region, Australia. *Geological Society of America Bulletin*, **113**, 1121–1132.

CORSETTI, F. A. & KAUFMAN, A. J. 2003. Stratigraphic investigations of carbon isotope anomalies and Neoproterozoic ice ages in Death Valley, California. *Geological Society of America Bulletin*, **115**, 916–932.

CORSETTI, F. A. & KAUFMAN, A. J. 2005. The relationship between the Neoproterozoic Noonday Dolomite and the Ibex Formation: new observations and their bearing on 'Snowball Earth'. *Earth-Science Reviews*, **73**, 63–78.

CORSETTI, F. A. & LORENTZ, N. J. 2006. On Neoproterozoic cap carbonates as chronostratigraphic markers. *In*: XIAO, S. & KAUFMAN, A. J. (eds) *Neoproterozoic Geobiology and Paleobiology*. Springer, New York, 273–294.

CORSETTI, F. A., STEWART, J. H. & HAGADORN, J. W. 2007. Neoproterozoic diamictite-cap carbonate succession and $\delta^{13}C$ chemostratigraphy from eastern Sonora, Mexico. *Chemical Geology*, **237**, 129–142.

DEMPSTER, T. J., ROGERS, G. *ET AL*. 2002. Timing of deposition, orogenesis and glaciation within the Dalradian rocks of Scotland: constraints from U–Pb zircon ages. *Journal of the Geological Society of London*, **159**, 83–94.

DENYSZYN, S. W., HALLS, H. C., DAVIS, D. W. & EVANS, D. A. D. 2009. Paleomagnetism and U–Pb geochronology of Franklin dykes in High Arctic Canada and Greenland: a revised age and paleomagnetic pole constraining block rotations in the Nares Strait region. *Canadian Journal of Earth Sciences*, **46**, 689–705.

EEROLA, T. 2006. Myöhäisproterotsooiset ilmastonmuutokset Tutkimuksia Etelä-Brasiliassa [Neoproterozoic climate changes; research on southern Brazil; Finnish with English abstract and bilingual figure captions]. *Geologi*, **58**, 164–174.

EMBLETON, B. J. J. & WILLIAMS, G. E. 1986. Low palaeolatitude of deposition for late Precambrian periglacial varvites in South Australia: implications for palaeoclimatology. *Earth and Planetary Science Letters*, **79**, 419–430.

EVANS, D. A. D. 2000. Stratigraphic, geochronological, and paleomagnetic constraints upon the Neoproterozoic climatic paradox. *American Journal of Science*, **300**, 347–433.

EVANS, D. A. D. 2003. A fundamental Precambrian–Phanerozoic shift in Earth's glacial style? *Tectonophysics*, **375**, 353–385.

EVANS, D. A. D. 2006. Proterozoic low orbital obliquity and axial-dipolar geomagnetic field from evaporite palaeolatitudes. *Nature*, **444**, 51–55.

EVANS, D. A. D., LI, Z. X., KIRSCHVINK, J. L. & WINGATE, M. T. D. 2000. A high-quality mid-Neoproterozoic paleomagnetic pole from the South China block, with implications for ice ages and the breakup configuration of Rodinia. *Precambrian Research*, **100**, 313–335.

EYLES, N. & JANUSZCZAK, N. 2004. 'Zipper-rift': a tectonic model for Neoproterozoic glaciations during the breakup of Rodinia after 750 Ma. *Earth-Science Reviews*, **65**, 1–73.

FAIRCHILD, I. J. & KENNEDY, M. J. 2007. Neoproterozoic glaciation in the Earth System. *Journal of the Geological Society of London*, **164**, 895–921.

FANG, W., VAN DER VOO, R. & JOHNSON, R. J. E. 1986. Eocambrian paleomagnetism of the Boston basin: evidence for displaced terrane. *Geophysical Research Letters*, **13**, 1450–1453.

FANNING, C. M. & LINK, P. K. 2004. U–Pb SHRIMP ages of Neoproterozoic (Sturtian) glaciogenic Pocatello Formation, southeastern Idaho. *Geology*, **32**, 881–884.

FANNING, C. M. & LINK, P. K. 2008. Age constraints for the Sturtian Glaciation; data from the Adelaide Geosyncline, South Australia and Pocatello Formation, Idaho, USA. *Geological Society of Australia Abstracts*, **91**, 57–62.

FISHER, N. I., LEWIS, T. & EMBLETON, B. J. J. 1987. *Statistical Analysis of Spherical Data*. Cambridge, Cambridge University Press.

FITZSIMONS, I. C. W. 2000. Grenville-age basement provinces in East Antarctica: evidence for three separate collisional orogens. *Geology*, **28**, 879–882.

FONT, E., TRINDADE, R. I. F. & NÉDÉLEC, A. 2005. Detrital remanent magnetization in haematite-bearing Neoproterozoic Puga cap dolostone, Amazon craton: a rock magnetic and SEM study. *Geophysical Journal International*, **163**, 491–500.

FONT, E., NÉDÉLEC, A., TRINDADE, R. I. F. & MOREAU, C. 2010. Fast or slow melting of the Marinoan Snowball Earth? The cap dolostone record. *Palaeogeography, Palaeoclimatology, Palaeoecology*, **295**, 215–225.

FRIMMEL, H. E. 2011. The Karoetjes Kop and Bloupoort Formations, Gifberg Group, South Africa, *In*: ARNAUD, E., HALVERSON, G. P. & SHIELDS-ZHOU, G. (eds) *The Geological Record of Neoproterozoic Glaciations*. Geological Society, London, Memoirs, **36**, 233–237.

FRIMMEL, H. E. & JIANG, S.-Y. 2001. Marine evaporites from an oceanic island in the Neoproterozoic Adamastor ocean. *Precambrian Research*, **105**, 57–71.

FRIMMEL, H. E., FÖLLING, P. G. & ERIKSSON, P. G. 2002. Neoproterozoic tectonic and climatic evolution recorded in the Gariep Belt, Namibia and South Africa. *Basin Research*, **14**, 55–67.

GALLET, Y., PAVLOV, V. & COURTILLOT, V. 2003. Magnetic reversal frequency and apparent polar wander of the Siberian platform in the earliest Palaeozoic, inferred from the Khorbusuonka river section (northeastern Siberia). *Geophysical Journal International*, **154**, 829–840.

GAUCHER, C. & POIRÉ, D. G. 2009. Palaeoclimatic events. Neoproterozoic–Cambrian evolution of the Río de la Plata Palaeocontinent. *In*: GAUCHER, C., SIAL, A. N., HALVERSON, G. P. & FRIMMEL, H. E. (eds) *Neoproterozoic–Cambrian Tectonics, Global Change and Evolution*. Elsevier, Amsterdam, Developments in Precambrian Geology, **16**, 123–130.

GAUCHER, C., FRIMMEL, H. E. & GERMS, G. J. B. 2009. Tectonic events and palaeogeographic evolution of southwestern Gondwana in the Neoproterozoic and Cambrian. *In*: GAUCHER, C., SIAL, A. N., HALVERSON, G. P. & FRIMMEL, H. E. (eds) *Neoproterozoic–Cambrian Tectonics, Global Change and Evolution*. Elsevier, Amsterdam, Developments in Precambrian Geology, **16**, 295–316.

GLADKOCHUB, D. P., WINGATE, M. T. D., PISAREVSKY, S. A., DONSKAYA, T. V., MAZUKABZOV, A. M., PONOMARCHUK, V. A. & STANEVICH, A. M. 2006. Mafic intrusions in southwestern Siberia and implications for a Neoproterozoic connection with Laurentia. *Precambrian Research*, **147**, 260–278.

GOODGE, J. W., MYROW, P., WILLIAMS, I. S. & BOWRING, S. A. 2002. Age and provenance of the Beardmore Group, Antarctica: constraints on Rodinia supercontinent breakup. *Journal of Geology*, **110**, 393–406.

GOSTIN, V. A., MCKIRDY, D. M., WEBSTER, L. J. & WILLIAMS, G. E. 2011. Mid-Ediacaran ice-rafting in the Adelaide Geosyncline and Officer Basin, South Australia. *In*: ARNAUD, E., HALVERSON, G. P. & SHIELDS-ZHOU, G. (eds) *The Geological Record of Neoproterozoic Glaciations*. Geological Society, London, Memoirs, **36**, 673–676.

GREY, K., HOCKING, R. M. *ET AL.* 2005. Lithostratigraphic nomenclature of the Officer Basin and correlative parts of the Paterson Orogen, Western Australia. *Western Australia Geological Survey, Report*, **93**, 89.

HAINES, P. W., HOCKING, R. M., GREY, K. & STEVENS, M. K. 2008. Vines 1 revisited: are older Neoproterozoic glacial deposits preserved in Western Australia? *Australian Journal of Earth Sciences*, **55**, 397–406.

HALVERSON, G. P., HOFFMAN, P. F., SCHRAG, D. P., MALOOF, A. C. & RICE, A. H. N. 2005. Toward a Neoproterozoic composite carbon-isotope record. *Geological Society of America Bulletin*, **117**, 1181–1207.

HALVERSON, G. P., DUDÁS, F. Ö., MALOOF, A. C. & BOWRING, S. A. 2007. Evolution of the $^{87}Sr/^{86}Sr$ composition of Neoproterozoic seawater. *Palaeogeography, Palaeoclimatology, Palaeoecology*, **256**, 103–129.

HAMBREY, M. J. & HARLAND, W. B. (eds) 1981. *Earth's Pre-Pleistocene Glacial Record*. Cambridge University Press, Cambridge, 1004.

HAMDI, B. 1992. Late Precambrian glacial deposits in central Iran. *29th International Geological Congress, Abstracts*, **2**, 232.

HANNAH, J., YANG, G., BINGEN, B., STEIN, H. & ZIMMERMAN, A. 2007. ~560 and ~300 Ma Re–Os ages constrain Neoproterozoic glaciation and record Variscan hydrocarbon migration on extension of Oslo rift. *In*: REDFIELD, T., BUITER, S. J. H. & SMETHURST, M. A. (eds) *geodynamics, Geomagnetism and Paleogeography: A 50 Year Celebration*. NGU Report 2007.057 (Trondheim: Geological Survey of Norway), 50.

HARTMANN, L. A., BITENCOURT, M. F., SANTOS, J. O. S., MCNAUGHTON, N. J., RIVERA, C. B. & BETIOLLO, L. 2003. Prolonged Paleoproterozoic magmatic participation in the Neoproterozoic Dom Feliciano belt, Santa Catarina, Brazil, based on zircon U–Pb SHRIMP geochronology. *Journal of South American Earth Sciences,* **16**, 477–492.

HEBERT, C. L., KAUFMAN, A. J., PENNISTON-DORLAND, S. C. & MARTIN, A. J. 2010. Radiometric and stratigraphic constraints on terminal Ediacaran (post-Gaskiers) glaciation and metazoan evolution. *Precambrian Research*, **182**, 402–412.

HODYCH, J. P. & COX, R. A. 2007. Ediacaran U–Pb zircon dates for the Lac Matapédia and Mt. St.-Anselme basalts of the Quebec Appalachians: support for a long-lived mantle plume during the rifting phase of Iapetus opening. *Canadian Journal of Earth Sciences*, **44**, 565–581.

HOFFMAN, P. F. 1999. The break-up of Rodinia, birth of Gondwana, true polar wander and the Snowball Earth. *Journal of African Earth Sciences*, **28**, 17–33.

HOFFMAN, P. F. 2009. Pan-glacial — a third state in the climate system. *Geology Today*, **25**, 107–114.

HOFFMAN, P. F. & SCHRAG, D. P. 2002. The Snowball Earth hypothesis: testing the limits of global change. *Terra Nova*, **14**, 129–155.

HOFFMAN, P. F. & LI, Z.-X. 2009. A palaeogeographic context for Neoproterozoic glaciation. *Palaeogeography, Palaeoclimatology, Palaeoecology*, **277**, 158–172.

HOFFMAN, P. F., HALVERSON, G. P., DOMACK, E. W., HUSSON, J. M., HIGGINS, J. A. & SCHRAG, D. P. 2007. Are basal Ediacaran (635

Ma) post-glacial 'cap dolostones' diachronous? *Earth and Planetary Science Letters*, **258**, 114–131.

HOFFMANN, K.-H., CONDON, D. J., BOWRING, S. A. & CROWLEY, J. L. 2004. U–Pb zircon date from the Neoproterozoic Ghaub Formation, Namibia: constraints on Marinoan glaciation. *Geology*, **32**, 817–820.

HUANG, B., XU, B., ZHANG, C., LI, Y. & ZHU, R. 2005. Paleomagnetism of the Baiyisi volcanic rocks (ca. 740 Ma) of Tarim, Northwest China: a continental fragment of Neoproterozoic Western Australia? *Precambrian Research*, **142**, 83–92.

HUCKRIEDE, R., KÜRSTEN, M. & VENZLAFF, H. 1962. Zur Geologie des Gebiets zwischen Kerman und Saghand (Iran). *Beihefte zum Geologischen Jahrbuch*, **51**, 197.

HYODO, H. & DUNLOP, D. J. 1993. Effect of anisotropy on the paleomagnetic contact test for a Grenville dike. *Journal of Geophysical Research*, **98**, 7997–8017.

IGLESIA-LLANOS, M. P., TAIT, J. A., POPOV, V. & ABALMASSOVA, A. 2005. Palaeomagnetic data from Ediacaran (Vendian) sediments of the Arkhangelsk region, NW Russia: an alternative apparent polar wander path of Baltica for the Late Proterozoic–Early Palaeozoic. *Earth and Planetary Science Letters*, **240**, 732–747.

INGLIS, J. D., MACLEAN, J. S., SAMSON, S. D., D'LEMOS, R. S., ADMOU, H. & HEFFERAN, K. 2004. A precise U–Pb zircon age for the Bleïda granodiorite, Anti-Atlas, Morocco: implications for the timing of deformation and terrane assembly in the eastern Anti-Atlas. *Journal of African Earth Sciences*, **39**, 277–283.

JANIKIAN, L., ALMEIDA, R. P. *ET AL.* 2008. The continental record of Ediacaran volcano-sedimentary successions in southern Brazil and their global implications. *Terra Nova*, **20**, 259–266.

JENKINS, R. J. F. 2011. Billy Springs glaciation, South Australia. *In*: ARNAUD, E., HALVERSON, G. P. & SHIELDS-ZHOU, G. (eds) *The Geological Record of Neoproterozoic Glaciations*. Geological Society, London, Memoirs, **36** 693–699.

KAMO, S. L. & GOWER, C. F. 1994. U–Pb baddeleyite dating clarifies age of characteristic paleomagnetic remanence of Long Range dykes, southeastern Labrador. *Atlantic Geology*, **30**, 259–262.

KAMO, S. L., GOWER, C. F. & KROGH, T. E. 1989. Birthdate for the Iapetus Ocean? A precise U–Pb zircon and baddeleyite age for the Long Range dikes, southeast Labrador. *Geology*, **17**, 602–605.

KAMO, S. L., KROGH, T. E. & KUMARAPELI, P. S. 1995. Age of the Grenville dyke swarm, Ontario-Quebec: implications for the timing of Iapetus rifting. *Canadian Journal of Earth Sciences*, **32**, 273–280.

KARLSTROM, K. E., BOWRING, S. A. *ET AL.* 2000. Chuar Group of the Grand Canyon: record of breakup of Rodinia, associated change in the global carbon cycle, and ecosystem expansion by 740 Ma. *Geology*, **28**, 619–622.

KAUFMAN, A. J., SIAL, A. N., FRIMMEL, H. E. & MISI, A. 2009. Neoproterozoic to Cambrian palaeoclimatic events in southwestern Gondwana. *In*: GAUCHER, C., SIAL, A. N., HALVERSON, G. P. & FRIMMEL, H. E. (eds) *Neoproterozoic–Cambrian Tectonics, Global Change and Evolution*. Elsevier, Amsterdam, Developments in Precambrian Geology, **16**, 369–388.

KAWAI, T., WINDLEY, B. F., TERABAYASHI, M., YAMAMOTO, H., ISOZAKI, Y. & MARUYAMA, S. 2008. Neoproterozoic glaciations in the mid-oceanic realm: an example from hemi-pelagic mudstones on Llanddwyn Island, Anglesey, U.K. *Gondwana Research*, **14**, 105–114.

KEMPF, O., KELLERHALS, P., LOWRIE, W. & MATTER, A. 2000. Paleomagnetic directions in Late Precambrian glaciomarine sediments of the Mirbat sandstone formation, Oman. *Earth and Planetary Science Letters*, **175**, 181–190.

KENDALL, B., CREASER, R. A., CALVER, C. R., RAUB, T. D. & EVANS, D. A. D. 2009. Correlation of Sturtian diamictite successions in southern Australia and northwestern Tasmania by Re–Os black shale geochronology and the ambiguity of 'Sturtian'-type diamictite–cap carbonate pairs as chronostratigraphic marker horizons. *Precambrian Research*, **172**, 301–310.

KENT, D. V. & DUPUIS, C. 2003. Paleomagnetic study of the Paleocene–Eocene Tarawan chalk and Esna shale: dual polarity remagnetizations of Cenozoic sediments in the Nile valley (Egypt). *Micropaleontology*, **49**, 139–146.

KEY, R. M., LIYUNGU, A. K., NJAMU, F. M., SOMWE, V. & BANDA, J. 2001. The western arm of the Lufilian Arc in NW Zambia and its

potential for copper mineralization. *Journal of African Earth Sciences*, **33**, 503–528.

KHOMENTOVSKY, V. V. 1986. The Vendian System of Siberia and a standard stratigraphic scale. *Geological Magazine*, **123**, 333–348.

KILNER, B., MAC NIOCAILL, C. & BRASIER, M. 2005. Low-latitude glaciation in the Neoproterozoic of Oman. *Geology*, **33**, 413–416.

KIRSCHVINK, J. L. 1978. The Precambrian-Cambrian boundary problem: paleomagnetic directions from the Amadeus Basin, Central Australia. *Earth and Planetary Science Letters*, **40**, 91–100.

KIRSCHVINK, J. L. 1992. Late Proterozoic low-latitude global glaciation: the Snowball Earth. *In*: SCHOPF, J. W. & KLEIN, C. C. (eds) *The Proterozoic Biosphere: A Multidisciplinary Study*. Cambridge University Press, Cambridge, 51–52.

KIRSCHVINK, J. L. & ROZANOV, A. YU. 1984. Magnetostratigraphy of Lower Cambrian strata from the Siberian platform: a paleomagnetic pole and a preliminary polarity time-scale. *Geological Magazine*, **121**, 189–203.

KRAVCHINSKY, V. A., KONSTANTINOV, K. M. & COGNÉ, J.-P. 2001. Palaeomagnetic study of Vendian and Early Cambrian rocks of South Siberia and Central Mongolia: was the Siberian platform assembled at this time? *Precambrian Research*, **110**, 61–92.

KRAVCHINSKY, V. A., SKLYAROV, E. V., GLADKOCHUB, D. P. & HARBERT, W. P. 2010. Paleomagnetism of the Precambrian Eastern Sayan rocks: implications for the Ediacaran–Early Cambrian paleogeography of the Tuva-Mongolian composite terrane. *Tectonophysics*, **486**, 65–80.

LEVASHOVA, N. M., KALUGIN, V. M., GIBSHER, A. S., YFF, J., RYABININ, A. B., MEERT, J. G. & MALONE, S. J. 2010. The origin of the Baydaric microcontinent, Mongolia: constraints from paleomagnetism and geochronology. *Tectonophysics*, **485**, 306–320.

LI, Y., LI, Y., SHARPS, R., MCWILLIAMS, M. & GAO, Z. 1991. Sinian paleomagnetic results from the Tarim block, western China. *Precambrian Research*, **49**, 61–71.

LI, Z.-X. 2000. New palaeomagnetic results from the 'cap dolomite' of the Neoproterozoic Walsh Tillite, northwestern Australia. *Precambrian Research*, **100**, 359–370.

LI, Z.-X. & EVANS, D. A. D. 2011. Late Neoproterozoic 40° intraplate rotation within Australia allows for a tighter-fitting and longer-lasting Rodinia. *Geology*, **39**, 39–42.

LINNEMANN, U., GERDES, A., DROST, K. & BUSCHMANN, B. 2007. The continuum between Cadomian orogenesis and opening of the Rheic Ocean: constraints from LA–ICP-MS U–Pb zircon dating and analysis of plate-tectonic setting (Saxo-Thuringian zone, northeastern Bohemian Massif, Germany. *In*: LINNEMANN, U., NANCE, R. D., KRAFT, P. & ZULAUF, G. (eds) *The Evolution of the Rheic Ocean: From Avalonian–Cadomian Active Margin to Alleghenian–Variscan Collision*. Geological Society of America, Special Paper, **423**, 61–96.

LUND, K., ALEINIKOFF, J. N. & EVANS, K. V. 2003. SHRIMP U–Pb geochronology of Neoproterozoic Windermere Supergroup, central Idaho: implications for rifting of western Laurentia and synchroneity of Sturtian glacial deposits. *Geological Society of America Bulletin*, **115**, 349–372.

MACOUIN, M., BESSE, J., ADER, M., GILDER, S., YANG, Z., SUN, Z. & AGRINIER, P. 2004. Combined paleomagnetic and isotopic data from the Doushantuo carbonates, South China: implications for the "Snowball Earth" hypothesis. *Earth and Planetary Science Letters*, **224**, 387–398.

MACDONALD, F. A., MCCLELLAND, W. C., SCHRAG, D. P. & MACDONALD, W. P. 2009*a*. Neoproterozoic glaciations on a carbonate platform margin in Arctic Alaska and the origin of the North Slope subterrane. *Geological Society of America Bulletin*, **121**, 448–473.

MACDONALD, F. A., JONES, D. S. & SCHRAG, D. P. 2009*b*. Stratigraphic and tectonic implications of a newly discovered glacial diamictite–cap carbonate couplet in southwestern Mongolia. *Geology*, **37**, 123–126.

MACDONALD, F. A., SCHMITZ, M. D. *ET AL.* 2010*a*. Calibrating the Cryogenian. *Science*, **327**, 1241–1243.

MACDONALD, F. A., COHEN, P. A., DUDÁS, F. Ö. & SCHRAG, D. P. 2010*b*. Early Neoproterozoic scale microfossils in the Lower Tindir Group of Alaska and the Yukon Territory. *Geology*, **38**, 143–146.

MACDONALD, F. A., STRAUSS, J. V., ROSE, C. V., DUDÁS, F. Õ. & SCHRAG, D. P. 2010*c*. Stratigraphy of the Port Nolloth Group of Namibia and South Africa and implications for the age of Neoproterozoic iron formations. *American Journal of Science*, **310**, 862–888.

MAC NIOCAILL, C., KILNER, B., STOUGE, S., KNUDSEN, M. F., HARPER, D. A. T. & CHRISTIANSEN, J. L. 2008. The Neoproterozoic drift history of Laurentia: a critical evaluation and new palaeomagnetic data from Northern and Eastern Greenland. *EOS Transactions of the American Geophysical Union*, **89**, S514–05.

MALOOF, A. C., SCHRAG, D. P., CROWLEY, J. L. & BOWRING, S. A. 2005. An expanded record of Early Cambrian carbon cycling from the Anti-Atlas Margin, Morocco. *Canadian Journal of Earth Sciences*, **42**, 2195–2216.

MARTIN, M. W., GRAZHDANKIN, D. V., BOWRING, S. A., EVANS, D. A. D., FEDONKIN, M. A. & KIRSCHVINK, J. L. 2000. Age of Neoproterozoic bilaterian body and trace fossils, White Sea, Russia: implications for metazoan evolution. *Science*, **288**, 841–845.

MBEDE, E. I., KAMPUNZU, A. B. & ARMSTRONG, R. A. 2004. Neoproterozoic inheritance during Cainozoic rifting in the western and southwestern branches of the East African rift system: evidence from carbonatite and alkaline intrusions. Conference abstract, The East African Rift System: Development, Evolution and Resources, Addis Ababa, Ethiopia, June 20–24, 2004.

MCCAUSLAND, P. J. A., VAN DER VOO, R. & HALL, C. M. 2007. Circum-Iapetus paleogeography of the Precambrian–Cambrian transition with a new paleomagnetic constraint from Laurentia. *Precambrian Research*, **156**, 125–152.

MCCAUSLAND, P. J. A., SMIRNOV, A., EVANS, D. A. D., IZARD, C. & RAUB, T. 2009. *Low-latitude Laurentia at 615 Ma: Paleomagnetism of the Long Range Dykes and Coeval Lighthouse Cove Formation, Northern Newfoundland and SE Labrador*. Abstracts, AGU-GAC/MAC-CGU Joint Assembly, Toronto, May 2009.

MCCAUSLAND, P. J. A., HANKARD, F., VAN DER VOO, R. & HALL, C. M. 2011. Ediacaran paleogeography of Laurentia: paleomagnetism and ^{40}Ar-^{39}Ar geochronology of the 583 Ma Baie des Moutons syenite, Quebec. *Precambrian Research*, **187**, 58–78.

MCCAY, G. A., PRAVE, A. R., ALSOP, G. I. & FALLICK, A. E. 2006. Glacial trinity: Neoproterozoic Earth history within the British-Irish Caledonides. *Geology*, **34**, 909–912.

MCFADDEN, P. L. & LOWES, F. J. 1981. The discrimination of mean directions drawn from Fisher distributions. *Geophysical Journal of the Royal Astronomical Society*, **67**, 19–33.

MCNAMARA, A. K., MAC NIOCAILL, C., VAN DER PLUIJM, B. A. & VAN DER VOO, R. 2001. West African proximity of the Avalon terrane in the latest Precambrian. *Geological Society of America Bulletin*, **113**, 1161–1170.

MCWILLIAMS, M. & SCHMIDT, P. W. 2003. *Paleomagnetism of Grassy Group rocks, King Island, Tasmania*. European Geophysical Society, Geophysical Research Abstracts, **5**, no. 12406.

MEERT, J. G. & VAN DER VOO, R. 1996. Paleomagnetic and ^{40}Ar/^{39}Ar study of the Sinyai Dolerite, Kenya: implications for Gondwana assembly. *Journal of Geology*, **104**, 131–142.

MEERT, J. G. & VAN DER VOO, R. 2001. Comment on 'New palaeomagnetic result from Vendian red sediments in Cisbaikalia and the problem of the relationship of Siberia and Laurentia in the Vendian' by S. A. Pisarevsky, R. A. Komissarova and A. N. Khramov. *Geophysical Journal International*, **146**, 867–870.

MEERT, J. G., VAN DER VOO, R. & PAYNE, T. W. 1994. Paleomagnetism of the Catoctin volcanic province: a new Vendian–Cambrian apparent polar wander path for North America. *Journal of Geophysical Research*, **99**, 4625–4641.

MEERT, J. G., VAN DER VOO, R. & AYUB, S. 1995. Paleomagnetic investigation of the Neoproterozoic Gagwe lavas and Mbozi complex, Tanzania and the assembly of Gondwana. *Precambrian Research*, **74**, 225–244.

MEERT, J. G., WALDERHAUG, H. J., TORSVIK, T. H. & HENDRIKS, B. W. H. 2007. Age and paleomagnetic signature of the Alnø carbonatite complex (NE Sweden): additional controversy for the Neoproterozoic paleoposition of Baltica. *Precambrian Research*, **154**, 159–174.

MEFFRE, S., DIREEN, N. G., CRAWFORD, A. J. & KAMENETSKY, V. 2004. Mafic volcanic rocks on King Island, Tasmania: evidence for 579 Ma break-up in east Gondwana. *Precambrian Research*, **135**, 177–191.

MELEZHIK, V. A., KUZNETSOV, A. B., FALLICK, A. F., SMITH, R. A., GOR-OKHOV, I. M., JAMAL, D. & CATUANE, F. 2006. Depositional environments and an apparent age for the Geci meta-limestones: constraints on the geological history of northern Mozambique. *Precambrian Research*, **148**, 19–31.

METELKIN, D. V., BELONOSOV, I. V., GLADKOCHUB, D. P., DONSKAYA, T. V., MAZUKABZOV, A. M. & STANEVICH, A. M. 2005. Paleomagnetic directions from Nersa intrusions of the Biryusa terrane, Siberian Craton, as a reflection of tectonic events in the Neoproterozoic. *Russian Geology and Geophysics*, **46**, 398–413.

MILLER, N. R., ALENE, M., SACCHI, R., STERN, R. J., CONTI, A., KRÖNER, A. & ZUPPI, G. 2003. Significance of the Tambien Group (Tigrai, N. Ethiopia) for Snowball Earth events in the Arabian–Nubian Shield. *Precambrian Research*, **121**, 263–283.

MISI, A., KAUFMAN, A. J. ET AL. 2007. Chemostratigraphic correlation of Neoproterozoic successions in South America. *Chemical Geology*, **237**, 143–167.

MITCHELL, R. N., EVANS, D. A. D. & KILIAN, T. M. 2010. Rapid Early Cambrian rotation of Gondwana. *Geology*, **38**, 755–758.

MUKHOPADHYAY, J. & CHAUDHURI, A. K. 2003. Shallow to deep-water deposition in a Cratonic basin: an example from the Proterozoic Penganga Group, Pranhita–Godavari Valley, India. *Journal of Asian Earth Sciences*, **21**, 613–622.

MURTHY, G. S. 1971. The paleomagnetism of diabase dikes from the Grenville Province. *Canadian Journal of Earth Sciences*, **8**, 802–812.

MURTHY, G., GOWER, C., TUBRETT, M. & PÄTZOLD, R. 1992. Paleomagnetism of Eocambrian Long Range dykes and Double Mer Formation from Labrador, Canada. *Canadian Journal of Earth Sciences*, **29**, 1224–1234.

MYROW, P. M., POPE, M. C., GOODGE, J. W., FISCHER, W. & PALMER, A. R. 2002. Depositional history of pre-Devonian strata and timing of Ross orogenic tectonism in the central Transantarctic Mountains, Antarctica. *Geological Society of America Bulletin*, **114**, 1070–1088.

NAWROCKI, J., BOGUCKIJ, A. & KATINAS, V. 2004. New Late Vendian palaeogeography of Baltica and the TESZ. *Geological Quarterly*, **48**, 309–316.

PAZOS, P. J., BETTUCCI, L. S. & LOUREIRO, J. 2008. The Neoproterozoic glacial record in the Río de la Plata Craton: a critical reappraisal. *In*: PANKHURST, R. J., TROUW, R. A. J., BRITO NEVES, B. B. & DE WIT, M. J. (eds) *West Gondwana: Pre-Cenozoic Correlations Across the South Atlantic Region*. Geological Society, London, Special Publication, **294**, 343–364.

PAZOS, P. J., SÁNCHEZ-BETTUCCI, L. & TOFALO, O. R. 2003. The record of the Varanger glaciation at the Río de la Plata craton, Vendian-Cambrian of Uruguay. *Gondwana Research*, **6**, 65–77.

PECOITS, E., GINGRAS, M., AUBET, N. & KONHAUSER, K. 2008. Ediacaran in Uruguay: palaeoclimatic and palaeobiological implications. *Sedimentology*, **55**, 689–719.

PINNA, P., JOURDE, G., CALVEZ, J. Y., MROZ, J. P. & MARQUES, J. M. 1993. The Mozambique Belt in northern Mozambique: Neoproterozoic (1100–850 Ma) crustal growth and tectogenesis, and superimposed Pan-African (800–550 Ma) tectonism. *Precambrian Research*, **62**, 1–59.

PISAREVSKY, S. A., KOMISSAROVA, R. A. & KHRAMOV, A. N. 2001. Reply to comment by J. G. Meert and R. Van der Voo on 'New palaeomagnetic result from Vendian red sediments in Cisbaikalia and the problem of the relationship of Siberia and Laurentia in the Vendian'. *Geophysical Journal International*, **146**, 871–873.

PISAREVSKY, S. A., WINGATE, M. T. D., STEVENS, M. K. & HAINES, P. W. 2007. Palaeomagnetic results from the Lancer 1 stratigraphic drillhole, Officer Basin, Western Australia, and implications for Rodinia reconstructions. *Australian Journal of Earth Sciences*, **54**, 561–572.

POIDEVIN, J.-L. 2007. Stratigraphie isotopique du strontium et datation des formations carbonatées et glaciogéniques néoprotérozoiques du Nord et de l'Ouest du craton du Congo. *Comptes Rendus Geoscience*, **339**, 259–273.

POIRÉ, D. G. & GAUCHER, C. 2009. Lithostratigraphy. Neoproterozoic–Cambrian evolution of the Río de la Plata Palaeocontinent. *In*: GAUCHER, C., SIAL, A. N., HALVERSON, G. P. & FRIMMEL, H. E. (eds) *Neoproterozoic–Cambrian Tectonics, global Change and Evolution*. Elsevier, Amsterdam, Developments in Precambrian Geology, **16**, 87–101.

POKROVSKII, B. G., MELEZHIK, V. A. & BUJAKAITE, M. I. 2006. Carbon, oxygen, strontium, and sulfur isotopic compositions in late Precambrian rocks of the Patom Complex, central Siberia: communication 1. results, isotope stratigraphy, and dating problems. *Lithology and Mineral Resources*, **41**, 450–474.

POPOV, V., IOSIFIDI, A., KHRAMOV, A., TAIT, J. & BACHTADSE, V. 2002. Paleomagnetism of Upper Vendian sediments from the Winter Coast, White Sea region, Russia: implications for the paleogeography of Baltica during Neoproterozoic times. *Journal of Geophysical Research*, **107**, doi: 10.1029/2001JB001607.

POPOV, V. V., KHRAMOV, A. N. & BACHTADSE, V. 2005. Palaeomagnetism, magnetic stratigraphy, and petromagnetism of the Upper Vendian sedimentary rocks in the sections of the Zolotitsa River and in the Verkhotina Hole, Winter Coast of the White Sea, Russia. *Russian Journal of Earth Sciences*, **7**, 1–29.

PORTER, S. M., KNOLL, A. H. & AFFATON, P. 2004. Chemostratigraphy of Neoproterozoic cap carbonates from the Volta Basin, West Africa. *Precambrian Research*, **130**, 99–112.

PRAVE, A. R. 1999. The Neoproterozoic Dalradian Supergroup of Scotland: an alternative hypothesis. *Geological Magazine*, **136**, 609–617.

RAMEZANI, J. & TUCKER, R. D. 2003. The Saghand region, central Iran: U–Pb geochronology, petrogenesis and implications for Gondwana tectonics. *American Journal of Science*, **303**, 622–665.

RAPALINI, A. E. & SÁNCHEZ-BETTUCCI, L. 2008. Widespread remagnetization of late Proterozoic sedimentary units of Uruguay and the apparent polar wander path for the Rio de La Plata craton. *Geophysical Journal International*, **174**, 55–74.

RAUB, T. D. 2008. *Prolonged deglaciation of Snowball Earth*. PhD thesis, Yale University.

RAUB, T. D., EVANS, D. A. D. & SMIRNOV, A. V. 2007a. Siliciclastic prelude to Elatina deglaciation: lithostratigraphy and rock magnetism of the base of the Ediacaran System. *In*: VICKERS-RICH, P. & KOMAROWER, P. (eds) *The Rise and Fall of the Ediacaran Biota*. Geological Society, London, Special Publication, **286**, 53–76.

RAUB, T. D., KIRSCHVINK, J. L. & EVANS, D. A. D. 2007b. True polar wander: linking deep and shallow geodynamics to hydro- and biospheric hypotheses. *In*: KONO, M. (ed.) *Treatise on Geophysics Volume 5: Geomagnetism*. Elsevier, Amsterdam, 565–589.

RIEU, R., ALLEN, P. A., COZZI, A., KOSLER, J. & BUSSY, F. 2007. A composite stratigraphy for the Neoproterozoic Huqf Supergroup of Oman: integrating new litho-, chemo- and chronostratigraphic data of the Mirbat area, southern Oman. *Journal of the Geological Society of London*, **164**, 997–1009.

RIEU, R., ALLEN, P. A., ETIENNE, J. L., COZZI, A. & WIECHERT, U. 2006. A Neoproterozoic glacially influenced basin margin succession and 'atypical' cap carbonate associated with bedrock palaeovalleys, Mirbat area, southern Oman. *Basin Research*, **18**, 471–496.

ROBERTS, D. 2003. The Scandinavian Caledonides: event chronology, palaeogeographic settings and likely modern analogues. *Tectonophysics*, **365**, 283–299.

RODRIGUES, J. B., PIMENTEL, M. M., BUHN, B., DARDENNE, M. A. & ALVARENGA, C. J. S. 2008. *Provenance of Vazante Group — Preliminary data*. VI South American Symposium on Isotope Geology, San Carlos de Bariloche, Argentina, 4.

ROONEY, A. D., SELBY, D., HOUZAY, J.-P. & RENNE, P. R. 2010. Re–Os geochronology of a Mesoproterozoic sedimentary succession, Taoudeni basin, Mauritania: implications for basin-wide correlations and Re–Os organic-rich sediments systematics. *Earth and Planetary Science Letters*, **289**, 486–496.

ROSE, C. V. & MALOOF, A. C. 2010. Testing models for post-glacial 'cap dolostone' deposition: Nuccaleena Formation, South Australia. *Earth and Planetary Science Letters*, **296**, 165–180.

ROWAN, C. J. & TAIT, J. 2010. *Oman's Low Latitude 'Snowball Earth' Pole Revisited: Late Cretaceous remagnetisation of Late Neoproterozoic Carbonates in Northern Oman*. American Geophysical Union, Fall Meeting Abstract GP33C-0959.

SÁNCHEZ-BETTUCCI, L. & RAPALINI, A. E. 2002. Paleomagnetism of the Sierra de Las Animas Complex, southern Uruguay: its implications in the assembly of western Gondwana. *Precambrian Research*, **118**, 243–265.

SCHMIDT, P. W. & WILLIAMS, G. E. 1995. The Neoproterozoic climatic paradox: equatorial palaeolatitude for Marinoan glaciation near sea level in South Australia. *Earth and Planetary Science Letters*, **134**, 107–124.

SCHMIDT, P. W., WILLIAMS, G. E. & EMBLETON, B. J. J. 1991. Low palaeolatitude of Late Proterozoic glaciation: early timing of remanence in haematite of the Elatina Formation, South Australia. *Earth and Planetary Science Letters*, **105**, 355–367.

SCHMIDT, P. W., WILLIAMS, G. E. & MCWILLIAMS, M. O. 2009. Palaeomagnetism and magnetic anisotropy of late Neoproterozoic strata, South Australia: implications for the palaeolatitude of late Cryogenian glaciation, cap carbonate and the Ediacaran System. *Precambrian Research*, **174**, 35–52.

SHEN, B., XIAO, S., ZHOU, C., KAUFMAN, A. J. & YUAN, X. 2010. Carbon and sulfur isotope chemostratigraphy of the Neoproterozoic Quanji Group of the Chaidam Basin, NW China: basin stratification in the aftermath of an Ediacaran glaciation postdating the Shuram event? *Precambrian Research*, **177**, 241–252.

SHIELDS, G. A., DEYNOUX, M., CULVER, S. J., BRASIER, M. D., AFFATON, P. & VANDAMME, D. 2007. Neoproterozoic glaciomarine and cap dolostone facies of the southwestern Taoudéni Basin (Walidiala Valley, Senegal/Guinea, NW Africa). *Comptes Rendus Geoscience*, **339**, 186–199.

SIAL, A. N., DARDENNE, M. A. *ET AL.* 2009. The São Francisco palaeocontinent. *In*: GAUCHER, C., SIAL, A. N., HALVERSON, G. P. & FRIMMEL, H. E. (eds) *Neoproterozoic–Cambrian Tectonics, Global Change and Evolution*. Elsevier, Amsterdam, Developments in Precambrian Geology, **16**, 31–69.

SOHL, L. E., CHRISTIE-BLICK, N. & KENT, D. V. 1999. Paleomagnetic polarity reversals in Marinoan (ca. 600 Ma) glacial deposits of Australia: implications for the duration of low-latitude glaciation in Neoproterozoic time. *Geological Society of America Bulletin*, **111**, 1120–1139.

SOVETOV, J. K. 2002. Vendian foreland basin of the Siberian cratonic margin: Paleopangean accretionary phases. *Russian Journal of Earth Sciences*, **4**, 363–387.

SOVETOV, J. 2008. *Marinoan Glaciation in the Siberian Craton: Locality, Erosional Forms, Deposits and Constraints to Age*. 33rd International Geological Congress, Abstracts, Session CGC-04.

SOVETOV, YU. K. & KOMLEV, D. A. 2005. Tillites at the base of the Oselok Group, foothills of the Sayan Mountains, and the Vendian lower boundary in the southwestern Siberian Platform. *Stratigraphy and Geological Correlation*, **13**, 337–366.

STERN, R. J., AVIGAD, D., MILLER, N. R. & BEYTH, M. 2006. Evidence for the Snowball Earth hypothesis in the Arabian–Nubian Shield and the East African Orogen. *Journal of African Earth Sciences*, **44**, 1–20.

SWANSON-HYSELL, N. L., MALOOF, A. C., WEISS, B. P. & & EVANS, D. A. D. 2009. No asymmetry in geomagnetic reversals recorded by 1.1-billion-year-old Keweenawan basalts. *Nature Geoscience*, **2**, 713–717.

TAUXE, L., KODAMA, K. P. & KENT, D. V. 2008. Testing corrections for paleomagnetic inclination error in sedimentary rocks: a comparative approach. *Physics of the Earth and Planetary Interiors*, **169**, 152–165.

THOMAS, R. J., CHEVALLIER, L. C. *ET AL.* 2002. Precambrian evolution of the Sirwa Window, Anti-Atlas Orogen, Morocco. *Precambrian Research*, **118**, 1–57.

THOMAS, R. J., FEKKAK, A. *ET AL.* 2004. A new lithostratigraphic framework for the Anti-Atlas Orogen, Morocco. *Journal of African Earth Sciences*, **39**, 217–226.

THOMPSON, M. D. & BOWRING, S. A. 2000. Age of the Squantum 'Tillite', Boston Basin, Massachusetts: U–Pb zircon constraints on terminal Neoproterozoic glaciation. *American Journal of Science*, **300**, 630–655.

THOMPSON, M. D., GRUNOW, A. M. & RAMEZANI, J. 2007. Late Neoproterozoic paleogeography of the southeastern New England Avalon zone: insights from U–Pb geochronology and paleomagnetism. *Geological Society of America Bulletin*, **119**, 681–696.

TOHVER, E., D'AGRELLA-FILHO, M. S. & TRINDADE, R. I. F. 2006. Paleomagnetic record of Africa and South America for the 1200–500 Ma interval, and evaluation of Rodinia and Gondwana assemblies. *Precambrian Research*, **147**, 193–222.

TORSVIK, T. H., LOHMANN, K. C. & STURT, B. A. 1995. Vendian glaciations and their relation to the dispersal of Rodinia: Paleomagnetic constraints. *Geology*, **23**, 727–730.

TRINDADE, R. I. F. & MACOUIN, M. 2007. Palaeolatitude of glacial deposits and palaeogeography of Neoproterozoic ice ages. *Comptes Rendus Geoscience*, **339**, 200–211.

TRINDADE, R. I. F., D'AGRELLA-FILHO, M. S., BABINSKI, M., FONT, E. & BRITO NEVES, B. B. 2004. Paleomagnetism and geochronology of the Bebedouro cap carbonate: evidence for continental-scale Cambrian remagnetization in the São Francisco craton, Brazil. *Precambrian Research*, **128**, 83–103.

TRINDADE, R. I. F., FONT, E., D'AGRELLA-FILHO, M. S., NOGUEIRA, A. C. R. & RICCOMINI, C. 2003. Low-latitude and multiple geomagnetic reversals in the Neoproterozoic Puga cap carbonate, Amazon craton. *Terra Nova*, **15**, 441–446.

TROMPETTE, R. 1994. *Geology of Western Gondwana (2000–500 Ma): Pan-African–Brasiliano Aggregation of South America and Africa*. Balkema, Rotterdam.

VAN DER VOO, R. 1990. The reliability of paleomagnetic data. *Tectonophysics*, **184**, 1–9.

VIZAN, H., CARNEY, J. N., TURNER, P., IXER, R. A., TOMASSO, M., MULLEN, R. P. & CLARKE, P. 2003. Late Neoproterozoic to Early Palaeozoic palaeogeography of Avalonia: some palaeomagnetic constraints from Nuneaton, central England. *Geological Magazine*, **140**, 685–705.

WEIL, A. B., GEISSMAN, J. W. & VAN DER VOO, R. 2004. Paleomagnetism of the Neoproterozoic Chuar Group, Grand Canyon Supergroup, Arizona: implications for Laurentia's Neoproterozoic APWP and Rodinia break-up. *Precambrian Research*, **129**, 71–92.

WILLIAMS, G. E. 1993. History of the Earth's obliquity. *Earth-Science Reviews*, **34**, 1–45.

WILLIAMS, G. E. 2008. Proterozoic (pre-Ediacaran) glaciation and the high obliquity, low-latitude ice, strong seasonality (HOLIST) hypothesis: principles and tests. *Earth-Science Reviews*, **87**, 61–93.

WILLIAMS, G. E., GOSTIN, V. A., MCKIRDY, D. M. & PREISS, W. V. 2008. The Elatina glaciation, late Cryogenian (Marinoan Epoch), South Australia: sedimentary facies and palaeoenvironments. *Precambrian Research*, **163**, 307–331.

XU, B., JIAN, P., ZHENG, H., ZOU, H., ZHANG, L. & LIU, D. 2005. U–Pb zircon geochronology and geochemistry of Neoproterozoic volcanic rocks in the Tarim Block of northwest China: implications for the breakup of Rodinia supercontinent and Neoproterozoic glaciations. *Precambrian Research*, **136**, 107–123.

XU, B., XIAO, S. *ET AL.* 2009. SHRIMP zircon U–Pb age constraints on Neoproterozoic Quruqtagh diamictites in NW China. *Precambrian Research*, **168**, 247–258.

ZHAN, S., CHEN, Y., XU, B., WANG, B. & FAURE, M. 2007. Late Neoproterozoic paleomagnetic results from the Sugetbrak Formation of the Aksu area, Tarim basin (NW China) and their implications to paleogeographic reconstructions and the Snowball Earth hypothesis. *Precambrian Research*, **154**, 143–158.

ZHANG, Q.-R. & PIPER, J. D. A. 1997. Palaeomagnetic study of Neoproterozoic glacial rocks of the Yangzi Block: palaeolatitude and configuration of South China in the late Proterozoic Supercontinent. *Precambrian Research*, **85**, 173–199.

ZHANG, Q.-R., LI, X.-H., FENG, L.-J., HUANG, J. & SONG, B. 2008. A new age constraint on the onset of the Neoproterozoic glaciations in the Yangtze Platform, South China. *Journal of Geology*, **116**, 423–429.

ZHANG, Q.-R., CHU, X. L. & FENG, L. J. 2009. Discussion on the Neoproterozoic glaciations in the South China Block and their related paleolatitudes. *Chinese Science Bulletin*, **54**, 1797–1800.

ZHANG, S., EVANS, D. A. D. *ET AL.* 2006. New paleomagnetic results from the Nantuo Formation in south China and their paleogeographic implications. *EOS, Transactions of the American Geophysical Union*, abstract GP34A-04.

ZHANG, S., JIANG, G. & HAN, Y. 2008. The age of the Nantuo Formation and Nantuo glaciation in South China. *Terra Nova*, **20**, 289–294.

ZHOU, C., TUCKER, R., XIAO, S., PENG, Z., YUAN, X. & CHEN, Z. 2004. New constraints on the ages of Neoproterozoic glaciations in south China. *Geology*, **32**, 437–440.